Calorie restriction protects against experimental abdominal aortic aneurysms in mice

Yue Liu,* Ting-Ting Wang,* Ran Zhang,* Wen-Yan Fu, Xu Wang, Fang Wang, Peng Gao, Yang-Nan Ding, Yan Xie, De-Long Hao, Hou-Zao Chen, and De-Pei Liu

State Key Laboratory of Medical Molecular Biology, Department of Biochemistry and Molecular Biology, Institute of Basic Medical Sciences, Chinese Academy of Medical Sciences and Peking Union Medical College, Beijing 100730, China

Abdominal aortic aneurysm (AAA), characterized by a localized dilation of the abdominal aorta, is a life-threatening vascular pathology. Because of the current lack of effective treatment for AAA rupture, prevention is of prime importance for AAA management. Calorie restriction (CR) is a nonpharmacological intervention that delays the aging process and provides various health benefits. However, whether CR prevents AAA formation remains untested. In this study, we subjected *Apoe*$^{-/-}$ mice to 12 wk of CR and then examined the incidence of angiotensin II (AngII)–induced AAA formation. We found that CR markedly reduced the incidence of AAA formation and attenuated aortic elastin degradation in *Apoe*$^{-/-}$ mice. The expression and activity of Sirtuin 1 (SIRT1), a key metabolism/energy sensor, were up-regulated in vascular smooth muscle cells (VSMCs) upon CR. Importantly, the specific ablation of SIRT1 in smooth muscle cells abolished the preventive effect of CR on AAA formation in *Apoe*$^{-/-}$ mice. Mechanistically, VSMC-SIRT1–dependent deacetylation of histone H3 lysine 9 on the *matrix metallopeptidase 2* (*Mmp2*) promoter was required for CR-mediated suppression of AngII-induced MMP2 expression. Together, our findings suggest that CR may be an effective intervention that protects against AAA formation.

INTRODUCTION

Abdominal aortic aneurysm (AAA) is a permanent, localized dilation of the abdominal aorta (Johnston et al., 1991). Mortality after AAA rupture can be as high as 80% (Logan and Bourantas, 2000; Verhoeven et al., 2008). Because of the lack of medical therapy, AAA treatment mainly consists of surgery when the dilation occurs quickly or reaches a diameter larger than 5.5 cm (Bown et al., 2013; Lederle, 2013). Thus, prevention is particularly important for AAA management. In addition to uncontrollable risk factors such as advancing age, male gender, and family history, controllable risk factors such as smoking and abdominal obesity greatly contribute to the onset of AAA (Nordon et al., 2011). Epidemiological studies have revealed that an increased waist-to-hip ratio is independently associated with AAA (Golledge et al., 2007; Stackelberg et al., 2013). Likewise, studies in mice have suggested that obese mice are more susceptible to AAA than lean mice (Police et al., 2009), and weight loss suppresses the expansion of established AAAs (Police et al., 2010). Although the development of AAA is related to metabolic disorders, it remains unknown whether improving systemic metabolism prevents the formation of AAA.

Calorie restriction (CR), which consists of decreasing caloric intake without causing malnutrition, is the only nonpharmacological intervention to slow the aging process in a wide variety of organisms ranging from yeast to primates (Piper and Bartke, 2008; Colman et al., 2009, 2014; Fontana et al., 2010). Studies on unconventional CR imply that CR may also reduce mortality in humans (Strom and Jensen, 1951; Willcox et al., 2007). Furthermore, cross-sectional studies and randomized controlled trials have demonstrated that CR effectively improves systemic metabolic parameters and prevents obesity and insulin resistance (Weiss et al., 2006; Fontana et al., 2007; Weiss and Holloszy, 2007). As a healthy food regimen, CR reduces risk factors of atherosclerosis and related cardiovascular diseases (CVDs) in humans (Fontana et al., 2004, 2007; Lefevre et al., 2009). Despite the metabolic and cardiovascular benefits of CR, whether CR represents an effective strategy for AAA prevention remains untested.

In the present study, we investigated the influence of CR on AAA formation in mice. We observed that CR significantly altered the systemic metabolic state of *Apoe*$^{-/-}$ mice and inhibited angiotensin II (AngII)–induced AAA formation in *Apoe*$^{-/-}$ mice. Notably, we observed a significant up-

*Y. Liu, T.-T. Wang, and R. Zhang contributed equally to this paper.

Correspondence to De-Pei Liu: liudp@pumc.edu.cn; or Hou-Zao Chen: chenhouzao@ibms.cams.cn

Y. Liu's present address is Dept. of Anesthesiology, China-Japan Friendship Hospital, Beijing 100029, China.

Abbreviations used: AAA, abdominal aortic aneurysm; AL, ad libitum; αSMA, α smooth muscle actin; AMPKα, AMP-activated protein kinase α; BW, body weight; ChIP, chromatin immunoprecipitation; CR, calorie restriction; CVD, cardiovascular disease; EE, energy expenditure; EVG, elastin van Gieson; eWAT, epididymal white adipose tissue; IF, immunofluorescence; IHC, immunohistochemistry; IPGTT, intraperitoneal glucose tolerance test; MMP, matrix metallopeptidase; mTOR, mechanistic target of rapamycin; NAD, nicotinamide adenine dinucleotide; RQ, respiratory quotient; SBP, systolic blood pressure; VSMC, vascular smooth muscle cell.

The Rockefeller University Press $30.00
J. Exp. Med. 2016 Vol. 213 No. 11 2473–2488
www.jem.org/cgi/doi/10.1084/jem.20151794

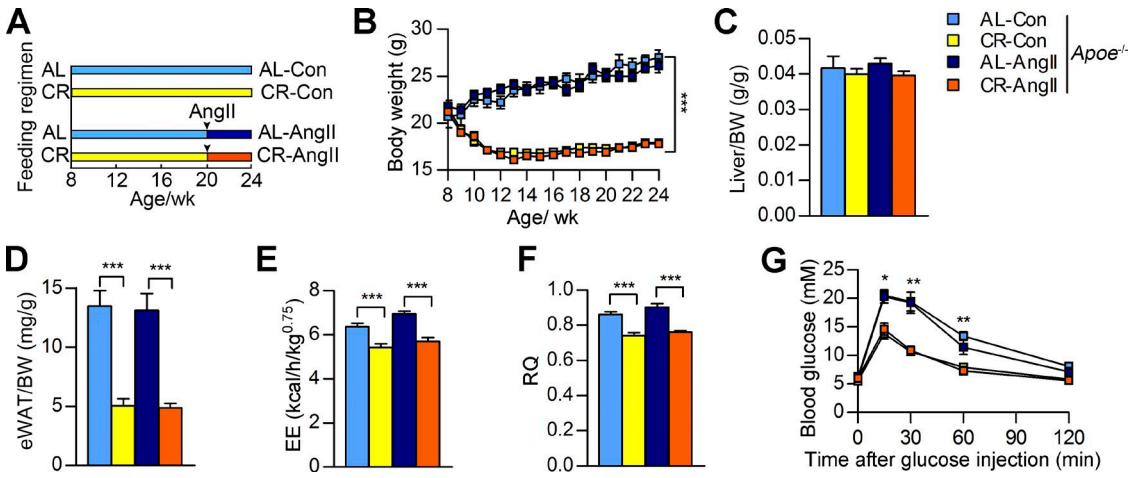

Figure 1. **Systemic metabolic indices of *Apoe*$^{-/-}$ mice after CR and AngII infusion.** (A) Schematic outlines of feeding and AngII infusion regimen for the four groups. (B) BW curve. n = 25–35 per group. (C and D) Liver weight–to-BW ratio (C) and eWAT weight–to-BW ratio (D) of *Apoe*$^{-/-}$ mice. n = 15–20 per group. (E and F) EE (E) and RQ (F) as measured by indirect calorimetry. n = 6–9 per group. (G) Blood glucose levels during IPGTT (2 g/kg). n = 5 per group. All values are shown as the means ± SEM. *, $P < 0.05$; **, $P < 0.01$; ***, $P < 0.001$. P-values were obtained using repeated measures ANOVA plus Tukey's multiple comparisons test (B and G), one-way ANOVA plus a Bonferroni test (C, E, and F), or a Kruskal-Wallis test plus a Dunn's multiple comparison test (D).

regulation of Sirtuin 1 (SIRT1) in vascular smooth muscle cells (VSMCs) under CR, and importantly, specific knockout ofVSMC-derived SIRT1 (VSMC-SIRT1) abolished the prevention of AAA by CR. These results revealed that SIRT1 in VSMCs plays a critical role in mediating the preventive effect of CR on AAA formation.

RESULTS

CR induces systemic metabolic changes in AngII-treated *Apoe*$^{-/-}$ mice

To investigate the influence of CR on AAA formation, *Apoe*$^{-/-}$ mice were calorie restricted or fed ad libitum (AL) for 12 wk, a strategy that has been widely used to investigate the effects of CR in mice (Hallows et al., 2011; Cerletti et al., 2012). After this 12-wk dietary intervention, mice in the experimental group received 4 wk of AngII infusion to induce AAA formation, whereas the control group received saline infusion (Fig. 1 A). During the experiment, AL mice displayed stable weight gain, whereas the weights of CR mice sharply decreased in the first 4 wk and then slightly increased in the remaining 12 wk (Fig. 1 B). However, no significant difference in body weight (BW) was observed between the AngII-infused mice and the control mice under the same dietary conditions. The liver weight–to-BW ratio was comparable in the four mouse groups (Fig. 1 C). Nonetheless, the epididymal white adipose tissue (eWAT)–to-BW ratio was markedly decreased after 16 wk of CR, notwithstanding that AngII infusion did not affect the eWAT-to-BW ratio (Fig. 1 D). These results indicate that CR constrains BW gain and fat storage in *Apoe*$^{-/-}$ mice.

We next examined the energy expenditure (EE) and respiratory quotient (RQ) of all groups of mice using indirect calorimetry. The results revealed that CR significantly reduced EE and decreased RQ in *Apoe*$^{-/-}$ mice, whereas AngII treatment did not notably affect the EE and RQ of *Apoe*$^{-/-}$ mice (Fig. 1, E and F), suggesting that CR mice tend to use more lipids rather than carbohydrates as an energy source compared with AL mice. We further examined systemic glucose and lipid metabolism in CR *Apoe*$^{-/-}$ mice. The fasting glucose levels were not significantly different between the four groups (Fig. 1 G). We analyzed the glucose regulatory function of these mice using an intraperitoneal glucose tolerance test (IPGTT). After glucose injection (2 g/kg BW), AL mice had higher increases in blood glucose levels than CR mice within 60 min, regardless of AngII treatment (Fig. 1 G), indicating that CR improves glucose tolerance in *Apoe*$^{-/-}$ mice. CR also notably decreased serum triglyceride levels in *Apoe*$^{-/-}$ mice, whereas AngII infusion did not affect the lipid profile of *Apoe*$^{-/-}$ mice (Table 1). Altogether, the results described in this section demonstrate that CR alters systemic metabolism in *Apoe*$^{-/-}$ mice, thus indicating the success of the mouse model construction for further analysis of the effect of CR on AAA formation.

CR reduces AngII-induced AAA formation

Apoe$^{-/-}$ mice with AngII infusion is a widely used animal model for AAA formation (Daugherty et al., 2000; Daugherty and Cassis, 2004). In the present study, AngII infusion increased systolic blood pressure (SBP) in both CR and AL mice, whereas CR had no notable effect on AngII-induced elevation of SBP (Table 1). There were no gross differences in morphology between the aortas of AL control (AL-Con; saline infusion) and CR-Con *Apoe*$^{-/-}$ mice (Fig. 2 A). 59% (29/49) of AL *Apoe*$^{-/-}$ mice developed AAA after AngII infusion, which is consistent with a previous study (Trivedi et al., 2013). In contrast, only 33% (11/33) of CR-AngII

Apoe$^{-/-}$ mice developed AAA (Fig. 2 C). Over the 4 wk of AngII infusion, 29% (14/49) of AL-AngII *Apoe*$^{-/-}$ mice died from aortic aneurysm rupture, whereas only 6% (2/33) of CR-AngII *Apoe*$^{-/-}$ mice died (Fig. 2 D).

AngII infusion markedly increased the aortic weight–to-BW ratio and maximal abdominal aortic diameter in *Apoe*$^{-/-}$ mice (Fig. 2, B and E). These effects were significantly alleviated by CR (Fig. 2, B and E). Elastin van Gieson (EVG) staining of the suprarenal aortas also demonstrated that the elastic lamina in the aortas of AL-Con and CR-Con *Apoe*$^{-/-}$ mice was intact and regularly arranged (Fig. 2, F and G). The aortic elastin was seriously degraded and disrupted in AL-AngII *Apoe*$^{-/-}$ mice, whereas the aortic elastin was more preserved in CR-AngII *Apoe*$^{-/-}$ mice compared with AL-AngII *Apoe*$^{-/-}$ mice (Fig. 2, F and G). Elastin is generated by medial VSMCs, and AAA is characterized by a loss of VSMCs (López-Candales et al., 1997). We therefore examined the density of VSMCs in the aortic media. Immunohistochemistry (IHC) of α smooth muscle actin (αSMA), a marker of VSMCs, in suprarenal aortas revealed that although there were no significant differences in VSMC density in the aortic media between the AL-Con and CR-Con *Apoe*$^{-/-}$ mice, the VSMC density in the aortic media was markedly lower in AL-AngII *Apoe*$^{-/-}$ mice compared with AL-Con *Apoe*$^{-/-}$ mice, and CR-AngII *Apoe*$^{-/-}$ mice had a higher VSMC density in the aortic media compared with AL-AngII *Apoe*$^{-/-}$ mice (Fig. 2, H and I). These observations suggested that CR alleviates the decrease in VSMC density caused by AngII infusion. In addition to elastin degradation and VSMC loss, AngII-induced cytokine expression and oxidative stress in the aortas of *Apoe*$^{-/-}$ mice were also reduced by CR (not depicted). Apart from AAAs induced by AngII infusion, consistent with a previous study (Daugherty et al., 2010), we observed that the maximal diameters of ascending aortas of *Apoe*$^{-/-}$ mice were markedly increased upon AngII infusion. Nevertheless, in the present study, the maximal diameters of ascending aortas of AL-AngII–treated *Apoe*$^{-/-}$ mice were comparable to those of CR-AngII–treated *Apoe*$^{-/-}$ mice (not depicted). Collectively, the results in this section suggest that a calorie-restricted diet effectively reduces the formation of AngII-induced AAAs and ameliorates the severity of AAAs in *Apoe*$^{-/-}$ mice.

CR does not affect the expression of genes involved in oxidative phosphorylation and glucose/lipid metabolism in aortas

Previous studies have revealed that the gene expression profiles in metabolic tissues, such as liver and skeletal muscle, are reprogrammed by CR in mice. The most significantly changed genes are involved in energy metabolism, which include oxidative phosphorylation, glucose metabolism, and lipid metabolism (Lee et al., 1999; Renaud et al., 2014). In the present study, we examined the metabolic state of the liver after 12-wk CR in the *Apoe*$^{-/-}$ mouse. We examined mRNA expression of *Ndufs8*, *Sdhb*, *Uqcrc1*, *Cox5b*, and *Atp5a1*, which encode the subunits of mitochondrial respiratory chain complexes I to V, respectively. The results demonstrated that the mRNA expression of these genes in the liver was significantly increased in response to CR (Fig. 3 A). Moreover, the mRNA expression levels of *Hk4* (a gene related to glycolysis) and *Pnpla2* (a gene related to lipolysis) in the liver were significantly increased in response to CR (Fig. 3 B). These results suggest that CR up-regulates the expression of oxidative respiratory chain complex genes and promotes glycolysis and lipolysis in the liver.

We next examined these metabolism-related indices in the aortas of *Apoe*$^{-/-}$ mice to investigate the downstream effectors in the aortas that mediate the effect of CR on AAA formation. In contrast to the liver, the mRNA expression levels of oxidative phosphorylation complexes in aortas were comparable between AL-Con and CR-Con *Apoe*$^{-/-}$ mice (Fig. 3 C). Furthermore, there were no significant differences in real-time PCR results for the aortic expression levels of genes related to glycolysis (e.g., *Hk1* and *Pkm*), fatty acid β-oxidation (e.g., *Cpt1a* and *Acadl*), lipolysis (e.g., *Lipe* and *Pnpla2*), and fatty acid synthesis (e.g., *Fasn*) between the AL-Con and CR-Con *Apoe*$^{-/-}$ mice (Fig. 3 D). All of these results indicated that CR does not significantly change the expression levels of oxidative phosphorylation complexes and the expression of genes related to glucose and lipid metabolism in aortas.

Table 1. **Serum lipid profile and SBP in *Apoe*$^{-/-}$ mice**

	AL-Con (n)	CR-Con (n)	AL-AngII (n)	CR-AngII (n)
TG (mmol/liter)	0.35 ± 0.03 (16)	0.17 ± 0.06[a] (13)	0.42 ± 0.04 (16)	0.08 ± 0.02[b] (15)
TC (mmol/liter)	11.05 ± 0.75 (16)	9.57 ± 0.64 (13)	10.84 ± 1.13 (16)	11.48 ± 1.07 (15)
HDL-C (mmol/liter)	0.51 ± 0.05 (16)	0.47 ± 0.04 (13)	0.56 ± 0.07 (16)	0.45 ± 0.03 (15)
LDL-C (mmol/liter)	2.5 ± 0.28 (16)	2.22 ± 0.14 (13)	2.29 ± 0.3 (16)	2.77 ± 0.28 (15)
SBP (mmHg)	108 ± 3.8 (10)	102.2 ± 3.9 (11)	134.2 ± 6.7[c] (9)	129.6 ± 6.5[d] (9)

The data are shown as the means ± SEM. Sample sizes (n) are shown in parenthesis. P-values were obtained using one-way ANOVA plus a posthoc analysis using a Bonferroni test in total cholesterol (TC) and SBP or by a Kruskal-Wallis test plus a posthoc analysis using a Dunn's multiple comparison test in triglyceride (TG), high-density lipoprotein-cholesterol (HDL-C), and low-density lipoprotein-cholesterol (LDL-C).

[a]$P < 0.05$ versus the AL-Con group.

[b]$P < 0.01$ versus the AL-AngII group.

[c]$P < 0.01$ versus the AL-Con group.

[d]$P < 0.01$ versus the CR-Con group.

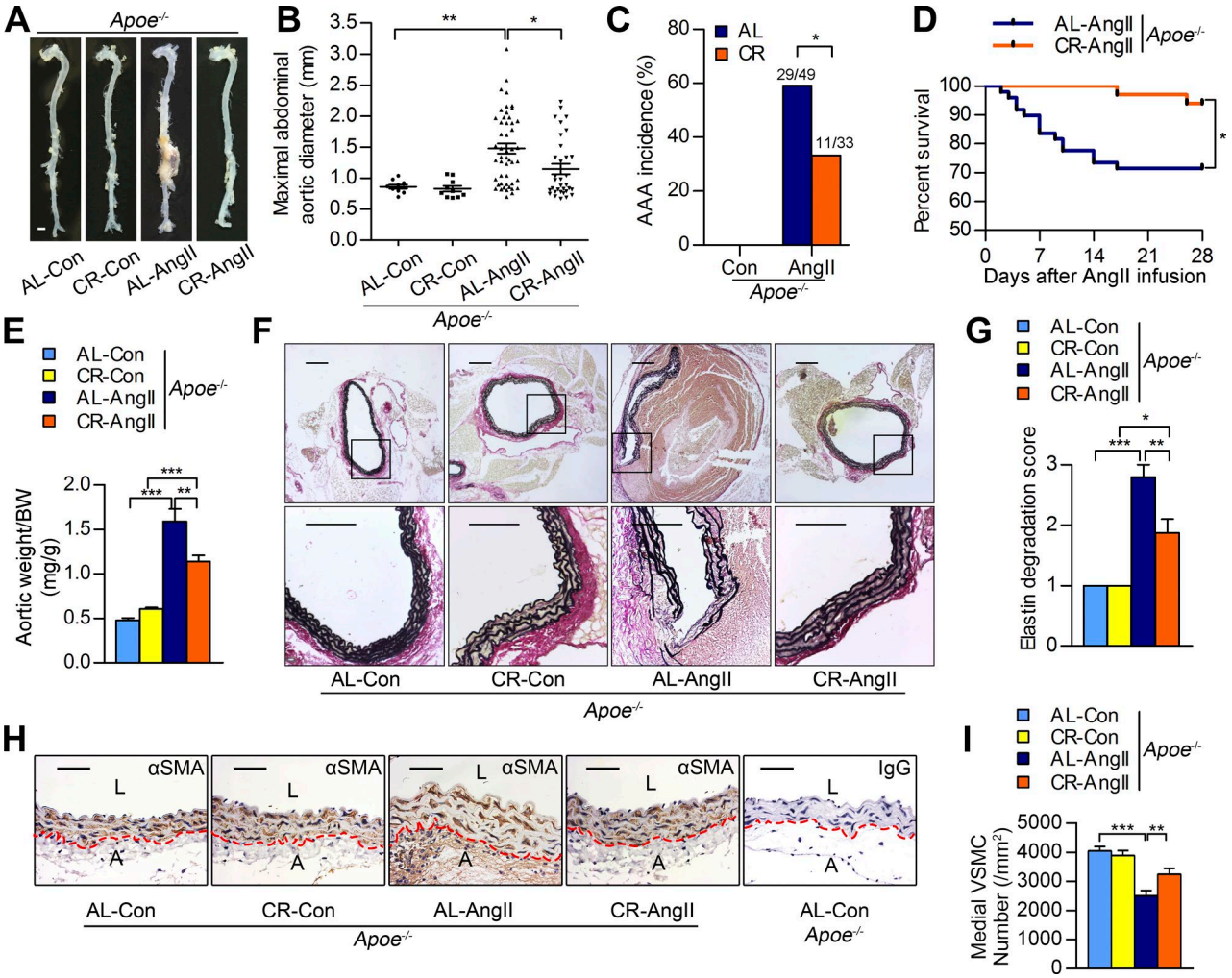

Figure 2. **CR reduces AngII-induced AAA formation in *Apoe*$^{-/-}$ mice.** (A) Representative images showing the macroscopic features of normal aortas and aneurysms of *Apoe*$^{-/-}$ mice in the indicated groups. Bar, 1 mm. (B) Maximal abdominal aortic diameter of *Apoe*$^{-/-}$ mice in the indicated groups. n = 10–49. (C and D) Incidence of AAAs (C) and survival curve (D) of *Apoe*$^{-/-}$ mice after AngII infusion. n = 49 in the AL-AngII group, and n = 33 in the CR-AngII group. (E) Total aortic weight-to-BW ratio of *Apoe*$^{-/-}$ mice in the indicated group. n = 27–30. (F and G) Representative images of EVG staining of abdominal aortic sections of *Apoe*$^{-/-}$ mice (F), and semiquantitative analysis of elastin degradation (G). Bars: (top) 200 µm; (bottom) 100 µm. n = 7–12. (H) IHC staining of αSMA in the suprarenal abdominal aortas of *Apoe*$^{-/-}$ mice in the indicated groups. Anti-αSMA antibody was replaced by normal IgG as a negative control. The demarcation between aortic media and adventitia is shown with red dotted lines. A, adventitia; L, lumen. Bar, 50 µm. (I) Quantification of αSMA-positive VSMC number per square millimeter in aortic media was calculated. n = 6–8. All values are shown as the means ± SEM. *, $P < 0.05$; **, $P < 0.01$; ***, $P < 0.001$. P-values were obtained using a Fisher's exact test (C), by a log-rank (Mantel-Cox) test (D), by a Kruskal-Wallis test plus a Dunn's multiple comparison test (B and E), or by one-way ANOVA plus a Bonferroni test (G and I).

VSMC-SIRT1 is the main sensor of CR in aortas

Metabolic/energy sensors, including SIRT1, SIRT3, AMP-activated protein kinase α (AMPKα), and mechanistic target of rapamycin (mTOR), have been reported to be involved in the response to CR in different contexts (Blagosklonny, 2010; Cantó and Auwerx, 2011; Guarente, 2013). To probe the mechanism of how CR protects against AAA formation, we examined the expression levels of these proteins in the aortas of 12-wk–CR *Apoe*$^{-/-}$ mice. Western blots demonstrated that SIRT1 protein expression was significantly up-regulated, whereas SIRT3 expression levels remained unchanged in the aortas of CR-Con *Apoe*$^{-/-}$ mice compared with AL-Con *Apoe*$^{-/-}$ mice (Fig. 4 A). Western blots also demonstrated that the total amounts of AMPKα and mTOR and their active forms (phosphorylated AMPKα and phosphorylated mTOR) did not change significantly in the aorta in response to CR (Fig. 4 A). In addition to SIRT1 protein levels, SIRT1 deacetylase activity also markedly increased in the aorta upon CR (Fig. 4 B). To determine the cell type in the aorta in which SIRT1 was up-regulated upon CR, we evaluated SIRT1 expression in VSMCs using immunofluorescence (IF). We observed that SIRT1 was mainly located in

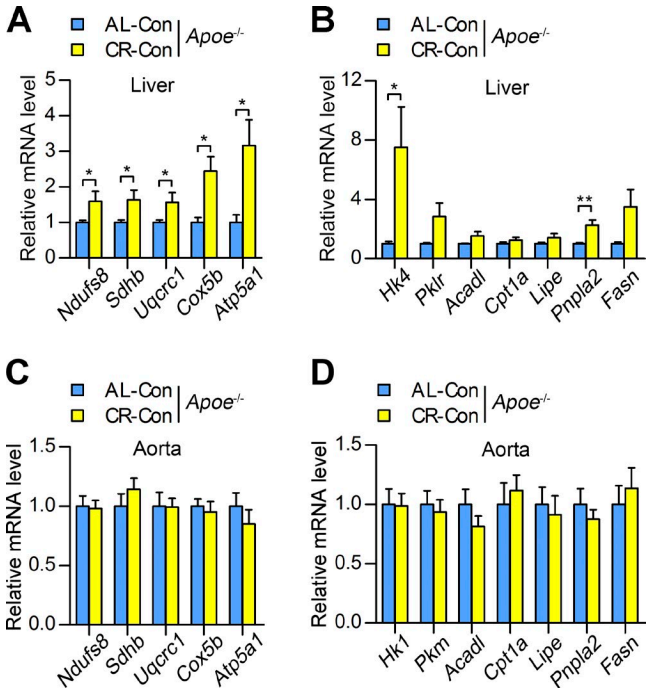

Figure 3. **Expression of genes involved in oxidative phosphorylation and glucose/lipid metabolism in the liver and aorta of *Apoe*$^{-/-}$ mice after 12 wk of CR.** (A) Relative mRNA expression of genes encoding mitochondrial respiratory chain subunits in *Apoe*$^{-/-}$ mouse livers. $n = 8$ per group. (B) Relative mRNA expression of genes involved in glucose and lipid metabolism in *Apoe*$^{-/-}$ mouse livers. $n = 8$ per group. (C and D) The relative mRNA expression of genes encoding mitochondrial respiratory chain subunits (C), and the genes involved in glucose and lipid metabolism (D) in the aortas of *Apoe*$^{-/-}$ mice. $n = 8$–12 per group. Three independent experiments were performed to obtain the data. All values are shown as the means ± SEM. *, $P < 0.05$; **, $P < 0.01$. P-values were obtained using an unpaired Student's *t* test with Welch's correction.

VSMCs (marked with αSMA), and SIRT1 expression in medial VSMCs increased after 12 wk of CR (Fig. 4 C). Although macrophages are also reportedly involved in AAA development (Longo et al., 2002; Wang et al., 2010), in the present study, there were few macrophages infiltrating the aortic walls after 12 wk of CR, as indicated by IHC for macrophages (Mac-3; not depicted). These results indicate that VSMC-SIRT1 plays a potentially important role in mediating the beneficial effects of CR in the aorta.

To further confirm the response of SIRT1 in VSMCs to CR, we conducted in vitro experiments using VSMCs isolated from the suprarenal region of abdominal aortas of *Apoe*$^{-/-}$ mice that were incubated with the serum of AL-Con or CR-Con *Apoe*$^{-/-}$ mice. Western blots demonstrated that SIRT1 expression was markedly increased in VSMCs incubated with the serum from CR-Con *Apoe*$^{-/-}$ mice for 48 h compared with those cells incubated with serum from AL-Con *Apoe*$^{-/-}$ mice. However, the expression levels of SIRT3, AMPKα, and mTOR, as well as AMPKα and mTOR, activities were not significantly changed in VSMCs after incubation with CR-Con *Apoe*$^{-/-}$ mouse serum (Fig. 4 D). Consistent with the in vivo findings, the mRNA levels of respiratory chain subunits and key enzymes involved in glucose and lipid metabolism were all comparable between the AL serum–incubated and CR serum–incubated VSMCs (Fig. 4, E and F). These results suggest that despite the unchanged metabolism in VSMCs, VSMC-SIRT1 is responsively up-regulated upon CR.

Ablation of SIRT1 in smooth muscle cells abolishes the preventive effect of CR on AAA formation

To investigate the role of VSMC-SIRT1 in mediating the protective effect of CR on AAA formation, we generated *Apoe*$^{-/-}$ mice that expressed a truncated and inactive form of SIRT1 specifically in smooth muscle cells (SVKO;*Apoe*$^{-/-}$ mice) using the *SM22α*–Cre mouse model, as previously described (Fig. 5, A and B; Gorenne et al., 2013). We observed that the WT SIRT1 protein was almost completely depleted, and a shorter truncated SIRT1 protein was expressed in the aorta of SVKO;*Apoe*$^{-/-}$ mice (Fig. 5, C and D). We performed the 12-wk CR followed by 4 wk of AngII infusion in these mice. We observed that CR decreased both BW (Fig. 5 E) and the eWAT weight–to-BW ratio (Fig. 5 F) but did not affect the liver weight–to-BW ratio (Fig. 5 G) in SVKO;*Apoe*$^{-/-}$ mice. EE and RQ decreased in response to CR in SVKO;*Apoe*$^{-/-}$ mice (Fig. 5, H and I). Blood triglyceride levels were also reduced by CR (Table 2). The blood glucose levels within 60 min after glucose challenge were significantly lower in the CR SVKO;*Apoe*$^{-/-}$ mice compared with AL SVKO;*Apoe*$^{-/-}$ mice (Fig. 5 J). These results suggest that smooth muscle–specific SIRT1 ablation does not affect the effects of CR on systemic metabolism, implicating that systemic metabolic changes lie upstream of the up-regulation of aortic SIRT1 expression in response to CR.

After AngII infusion, 70% (14/20) of AL *Sirt1*$^{flox/flox}$;*Apoe*$^{-/-}$ mice and 32% (6/19) of CR *Sirt1*$^{flox/flox}$;*Apoe*$^{-/-}$ mice developed AAAs (Fig. 6, A–C). However, the incidence of AAA was 64% (16/25) for AL-AngII SVKO;*Apoe*$^{-/-}$ mice and 71% (15/21) for CR-AngII SVKO;*Apoe*$^{-/-}$ mice, which were not remarkably different (Fig. 6, A–C). Furthermore, CR reduced AngII-induced mortalities in *Sirt1*$^{flox/flox}$;*Apoe*$^{-/-}$ mice, whereas the mortalities caused by aortic rupture in AL-AngII and CR-AngII SVKO;*Apoe*$^{-/-}$ mice were also not significantly different (Fig. 6 D). AngII infusion caused a notable increase in the total aortic weight–to-BW ratio and the aortic maximal diameter in both AL and CR groups of SVKO;*Apoe*$^{-/-}$ mice (Fig. 6, B and E). No significant differences were observed in these indices between the AL-AngII and CR-AngII SVKO;*Apoe*$^{-/-}$ mice (Fig. 6, B and E). In addition, there was no significant difference between the maximal diameters of ascending aortas of the AL and CR groups of SVKO;*Apoe*$^{-/-}$ mice upon AngII infusion (not depicted). EVG staining results showed that CR preserved elastin degradation in *Sirt1*$^{flox/flox}$;*Apoe*$^{-/-}$ mice after AngII administration. However, there

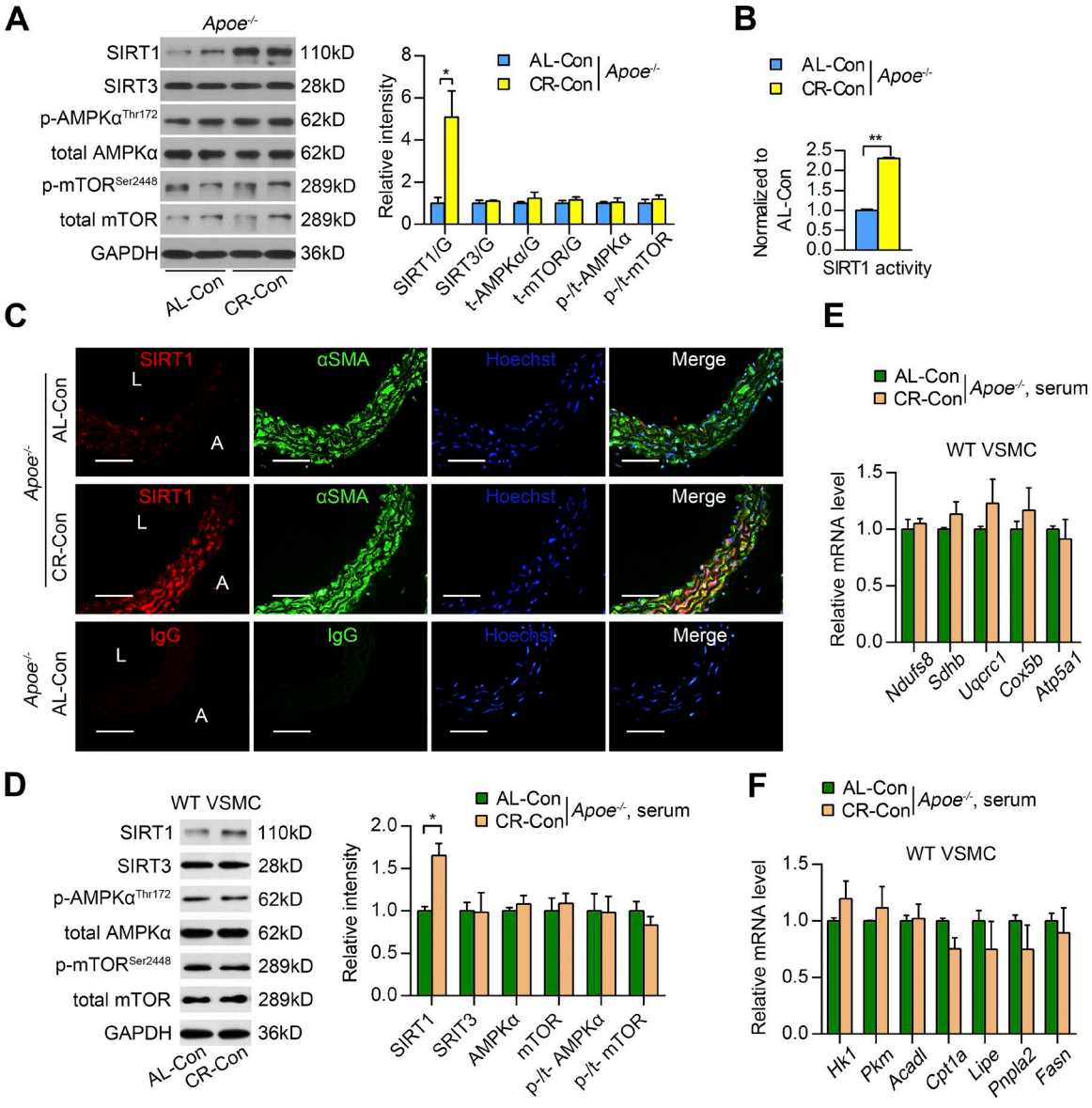

Figure 4. **VSMC-SIRT1 is the main sensor of CR in aortas.** (A) SIRT1, SIRT3, phosphorylated (p-AMPKα) and total AMPKα (t-AMPKα), and phosphorylated (p-mTOR) and total mTOR (t-mTOR) protein expression in aortas of *Apoe*$^{-/-}$ mice in the indicated group. Protein expression was detected by Western blotting (left) and quantified by densitometry (right). Quantitative results are normalized to the AL-Con group values. $n = 5$ per group. G, GAPDH. (B) SIRT1 activity in aortas of *Apoe*$^{-/-}$ mice from the indicated group. $n = 5$ per group. (C) Representative images of IF staining of SIRT1, VSMCs (αSMA), and nuclei (Hoechst) in the suprarenal aortas of *Apoe*$^{-/-}$ mice for the indicated groups. Anti-SIRT1 and anti-αSMA antibodies were replaced by normal IgG as a negative control. A, adventitia; L, lumen. Bars, 50 µm. (D) SIRT1, SIRT3, phosphorylated and total AMPKα, and phosphorylated and total mTOR protein expression in VSMCs (isolated from the suprarenal abdominal aortas of WT mice) that were incubated with serum from AL-Con mice or CR-Con mice for 48 h. Protein expression was detected by Western blotting (left) and quantified by densitometry (right). Quantitative results are normalized to the values of the AL-Con group. Experiments were performed in triplicate. (E and F) Relative mRNA expression of genes encoding mitochondrial respiratory chain subunits (E) and genes involved in glucose and lipid metabolism (F) in WT VSMCs that were incubated with serum from AL-Con mice or CR-Con mice for 48 h. Experiments were performed in triplicate. All values are shown as the means ± SEM. *, $P < 0.05$; **, $P < 0.01$. P-values were obtained using an unpaired Student's *t* test with Welch's correction.

were no differences in the degree of elastin degradation in SVKO;*Apoe*$^{-/-}$ mice in either the AL-AngII or CR-AngII groups (Fig. 6, F and G). All of these results suggest that the preventive effect of CR on AngII-induced AAA formation was reduced by VSMC-SIRT1 ablation.

CR attenuates AngII-induced matrix metallopeptidase 2 (MMP2) expression through epigenetic chromatin modification

Extracellular matrix degradation plays a critical role in AAA formation, and MMP2 and MMP9 are particularly import-

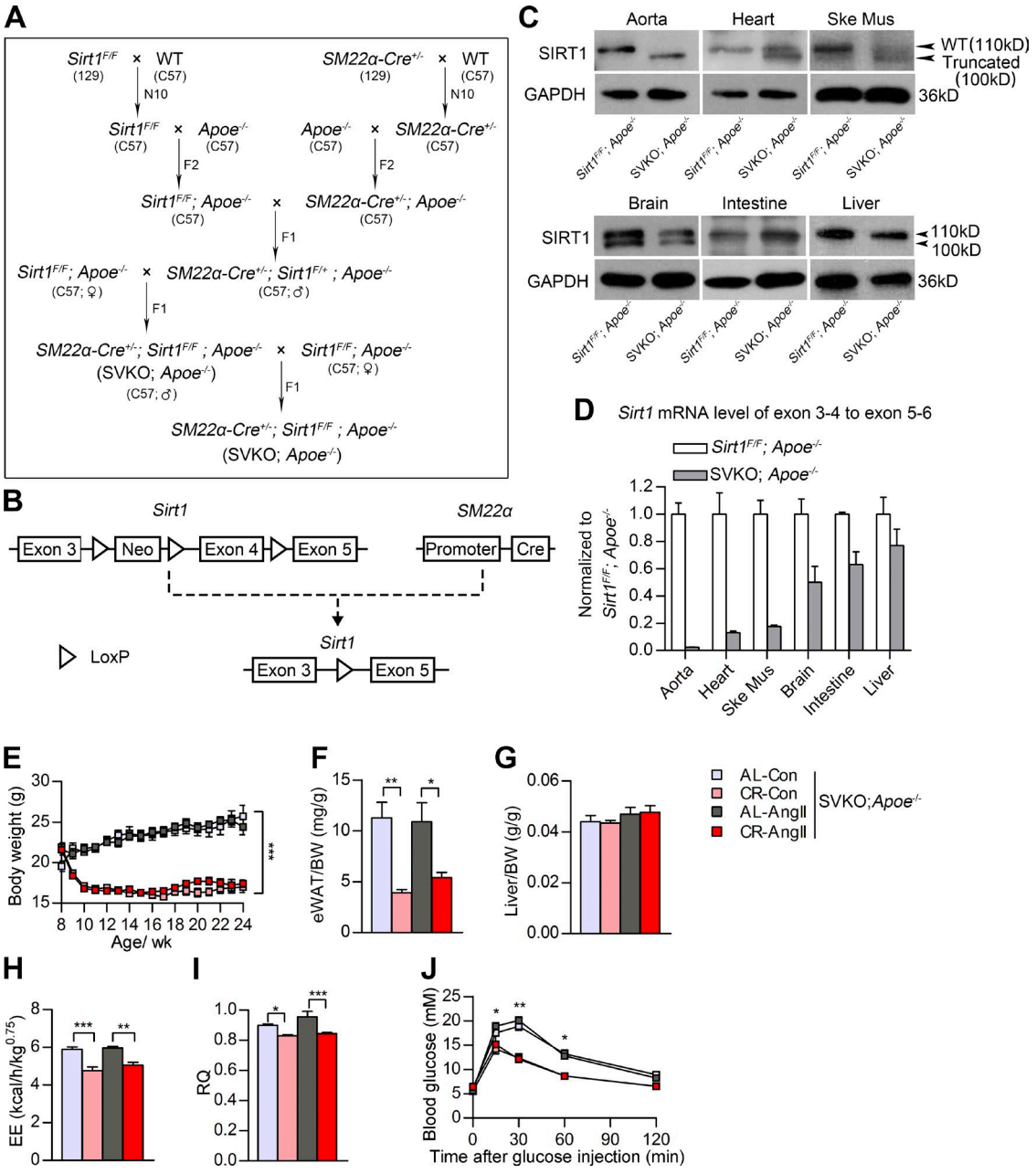

Figure 5. **Systemic metabolic indices of smooth muscle–specific *Sirt1* KO (SVKO;*Apoe*$^{-/-}$) mice after CR and AngII infusion.** (A) Breeding strategy to generate SVKO;*Apoe*$^{-/-}$ mice. F, filial generations; N, number of backcross generations. (B) The design of a Cre/LoxP system to delete the SIRT1 deacetylase domain, which is encoded by exon 4, in mouse smooth muscle cells. Neo, neomycin. (C) Western blots of SIRT1 in the aorta, heart, skeletal muscle (Ske Mus), brain, small intestine, and liver of WT (*Sirt1*$^{flox/flox}$;*Apoe*$^{-/-}$) and SVKO;*Apoe*$^{-/-}$ mice as indicated. (D) Real-time PCR quantification of exons 3–4 of SIRT1 mRNA in different tissues of SVKO mice. All SIRT1 exon 3–4 mRNA expression levels were normalized to SIRT1 exon 5–6 levels. Experiments were performed with three biological replicates. Primer sets used in real-time PCR are provided in Table S2. (E) BW curve of SVKO;*Apoe*$^{-/-}$ mice. n = 10 in the AL-Con, 10 in the CR-Con, 19 in the AL-AngII, and 21 in the CR-AngII groups. (F and G) The eWAT weight–to-BW ratio (F) and liver weight–to-BW ratio (G) of SVKO;*Apoe*$^{-/-}$ mice. n = 7–10 per group. (H and I) EE (H) and RQ (I) of SVKO;*Apoe*$^{-/-}$ mice as measured by indirect calorimetry. n = 4–5 per group. (J) Blood glucose levels during IPGTT (2 g/kg). n = 5 per group. All values are shown as the means ± SEM. *, $P < 0.05$; **, $P < 0.01$; ***, $P < 0.001$. P-values were obtained using two-way repeated-measures ANOVA (E and J), by a Kruskal-Wallis test plus a Dunn's multiple comparison test (F), or by one-way ANOVA plus a Bonferroni posthoc analysis (G–I).

ant in this process (Longo et al., 2002). We examined the effect of CR on the expression and activities of MMP2 and MMP9 in the aortas of *Apoe*$^{-/-}$ mice. There were no significant differences in the protein and mRNA levels of MMP2 and MMP9 between the AL-Con and CR-Con *Apoe*$^{-/-}$ mouse aortas (Fig. 7, A and C). However, compared with AL-Con *Apoe*$^{-/-}$ mice, there was a dramatic up-regulation of MMP2 and MMP9 protein and mRNA levels in the aortas of AL-AngII *Apoe*$^{-/-}$ mice; this up-regulation was significantly suppressed in the aortas of CR-AngII *Apoe*$^{-/-}$ mice compared with AL-AngII *Apoe*$^{-/-}$ mice (Fig. 7, A and C). Consistently, gelatin zymography demonstrated lower MMP2 activity in the aortas of CR-AngII *Apoe*$^{-/-}$ mice compared with AL-AngII *Apoe*$^{-/-}$ mice (Fig. 7 B). Particularly, MMP2 showed remarkably higher expression levels and activity compared with MMP9 (Fig. 7, B and C), suggesting that MMP2 is the predominant MMP in aortas. We therefore examined *Mmp2* mRNA levels in the aortas of SVKO;*Apoe*$^{-/-}$ mice by quantitative real-time PCR. The results demonstrated that the AngII-induced up-regulation of *Mmp2* expression was not attenuated by CR in SVKO;*Apoe*$^{-/-}$ mice (Fig. 7 D), indicating that CR inhibits AngII-induced MMP2 expression in a VSMC-SIRT1–dependent manner.

We next investigated the mechanism by which SIRT1 regulates MMP2 expression during CR. SIRT1 is a histone H3 lysine 9 (H3K9) and H4K16 deacetylase (Vaquero et al., 2004), and studies have demonstrated that the subtle enhancement of histone acetylation in the promoter can increase target gene transcription (Taylor et al., 2013; Ryall et al., 2015). Therefore, we analyzed the histone acetylation state in the aortas of *Apoe*$^{-/-}$ and SVKO;*Apoe*$^{-/-}$ mice in response to CR. Western blots demonstrated that the overall H3K9 and H4K16 acetylation (H3K9ac and H4K16ac) levels in *Apoe*$^{-/-}$ mouse aortas were not significantly changed upon CR either with or without AngII infusion (Fig. 8 A). Moreover, CR and AngII infusion did not change the overall H3K9 and H4K16 acetylation levels in aortas when SIRT1 was ablated (Fig. 8 A). Thus, we performed chromatin immunoprecipitation (ChIP) followed by quantitative PCR using mouse aortas with antibodies against H3K9ac and H4K16ac to examine whether CR affected the in vivo H3K9ac and H4K16ac levels on the *Mmp2* promoter. Specific primers complementary to the regions at −919 to −784 bp, −669 to −485 bp, −404 to −261 bp, and −260 to −105 bp in the *Mmp2* promoter were designed. The results demonstrated that both H3K9ac and H4K16ac levels were significantly higher than normal IgG on the four regions of the *Mmp2* promoter, but no significant differences in the H3K9ac and H4K16ac levels were observed among the four *Mmp2* promoter regions in the aortas of *Apoe*$^{-/-}$ mice (Fig. 8, B and C). ChIP assay results further showed that CR did not markedly influence H4K16ac or H3K9ac levels on the *Mmp2* promoter without AngII infusion in the aortas of *Apoe*$^{-/-}$ mice (Fig. 8, D and E). However, H3K9ac levels on the *Mmp2* promoter were remarkably increased upon AngII stimulation. After the treatment of AngII, CR significantly reduced H3K9ac levels in the regions of −919 to −784 bp, −669 to −485 bp, and −260 to −105 bp on the *Mmp2* promoter in the aortas of *Apoe*$^{-/-}$ mice (Fig. 8 D), whereas H4K16ac levels in the *Mmp2* promoter were not significantly affected by CR even in AngII-treated *Apoe*$^{-/-}$ mice (Fig. 8 E). Hence, these results indicate that CR specifically prevents the increase of AngII-induced H3K9ac on the *Mmp2* promoter.

To investigate whether SIRT1 mediates the suppressive effect of CR on AngII-induced H3K9ac increase, the aortas of AngII-treated SVKO;*Apoe*$^{-/-}$ mice were used for H3K9ac ChIP assay. The results showed that CR did not significantly change H3K9ac levels on the *Mmp2* promoter in AngII-treated SVKO;*Apoe*$^{-/-}$ mice (Fig. 8 D). Hence, VSMC-SIRT1 is required for the prevention of AngII-induced H3K9ac increase on the *Mmp2* promoter. We next examined the expression and activity of SIRT1 upon AngII infusion. The results showed that, although AngII infusion did not significantly affect SIRT1 expression, AngII treatment decreased SIRT1 deacetylase activity and nicotinamide adenine dinucleotide (NAD^+) availability in the aortas of *Apoe*$^{-/-}$

Table 2. **Serum lipid profile and SBP of *Sirt1*$^{flox/flox}$;*Apoe*$^{-/-}$ and SVKO;*Apoe*$^{-/-}$ mice**

Mice group	*Sirt1*$^{flox/flox}$;*Apoe*$^{-/-}$		SVKO;*Apoe*$^{-/-}$			
	AL-AngII	CR-AngII	AL-Con	CR-Con	AL-AngII	CR-AngII
TG (mmol/liter)	0.45 ± 0.1 (6)	0.07 ± 0.03[a] (6)	0.42 ± 0.04 (8)	0.15 ± 0.08[b] (9)	0.43 ± 0.06 (8)	0.18 ± 0.04[c] (9)
TC (mmol/liter)	10.02 ± 1.09 (6)	10.98 ± 1.47 (6)	11.2 ± 0.52 (8)	12.58 ± 1.04 (9)	11.77 ± 1.48 (8)	11.57 ± 0.74 (9)
HDL-C (mmol/liter)	0.5 ± 0.09 (6)	0.46 ± 0.05 (6)	0.52 ± 0.05 (8)	0.53 ± 0.04 (9)	0.52 ± 0.07 (8)	0.56 ± 0.05 (9)
LDL-C (mmol/liter)	2.701 ± 0.27 (6)	2.42 ± 0.45 (6)	2.34 ± 0.18 (8)	2.93 ± 0.2 (9)	2.51 ± 0.3 (8)	2.81 ± 0.16 (9)
SBP (mmHg)	130.9 ± 6.1 (6)	126.2 ± 7.1 (8)	92.8 ± 3.4 (8)	100.7 ± 2.3 (10)	127.4 ± 7.2[d] (9)	126 ± 6.1[e] (11)

The data are shown as the means ± SEM. Sample sizes (n) are shown in parenthesis. P-values were obtained using one-way ANOVA plus a posthoc analysis using a Bonferroni test in triglyceride (TG), total cholesterol (TC), high-density lipoprotein-cholesterol (HDL-C), and low-density lipoprotein-cholesterol (LDL-C) or a Kruskal-Wallis test plus a posthoc analysis using a Dunn's multiple comparison test in SBP.

[a]P < 0.05 versus AL-AngII group of *Sirt1*$^{flox/flox}$;*Apoe*$^{-/-}$ mice.

[b]P < 0.01 versus AL-Con group of SVKO;*Apoe*$^{-/-}$ mice.

[c]P < 0.01 versus AL-AngII group of SVKO;*Apoe*$^{-/-}$ mice.

[d]P < 0.01 versus the AL-Con group of SVKO;*Apoe*$^{-/-}$ mice.

[e]P < 0.01 versus the CR-Con group of SVKO;*Apoe*$^{-/-}$ mice.

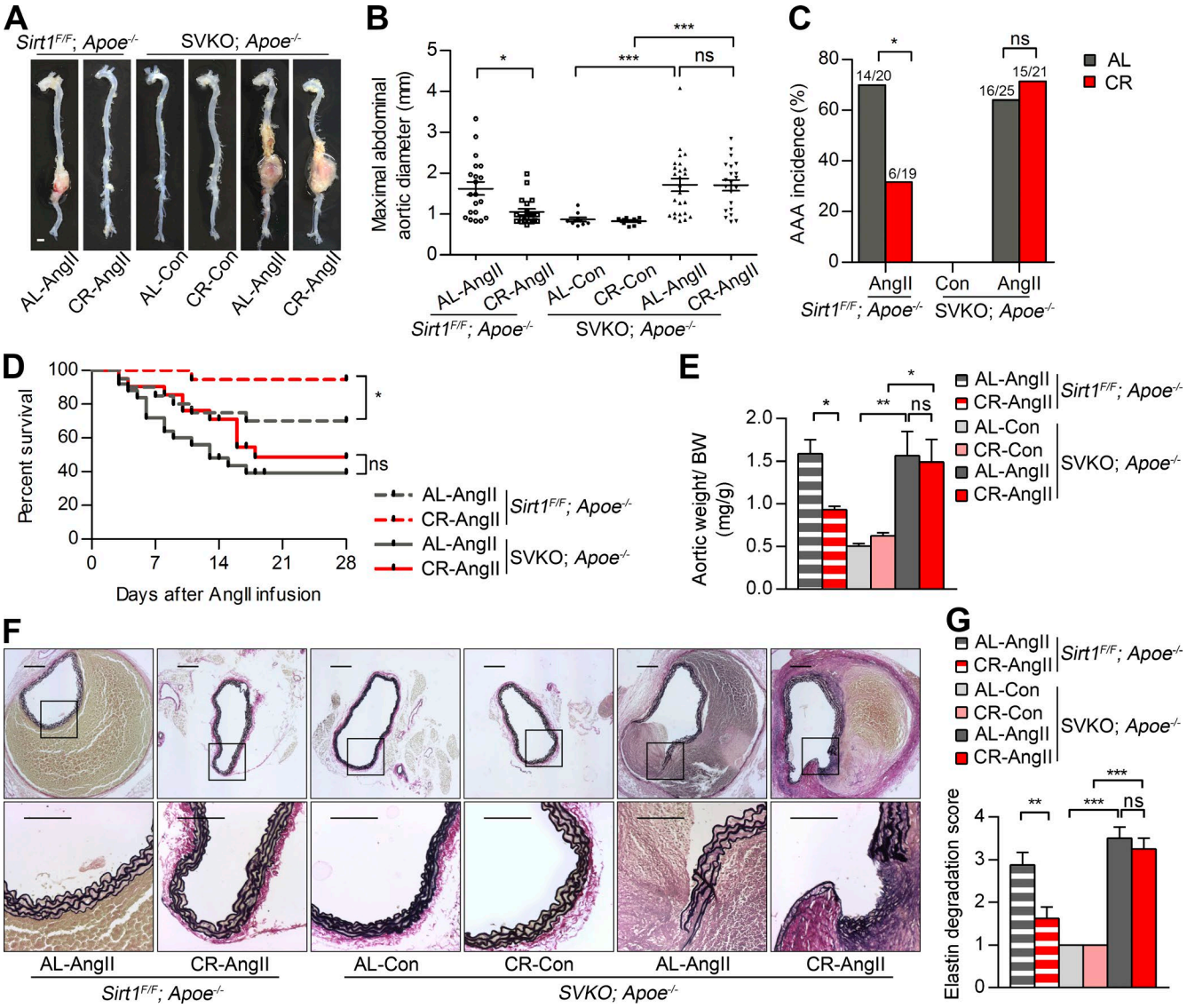

Figure 6. **SIRT1 ablation in VSMCs abolished the preventive effect of CR on AAA formation.** (A) Representative images showing the macroscopic features of normal aortas and aneurysms of *Sirt1*$^{flox/flox}$;*Apoe*$^{-/-}$ mice and SVKO;*Apoe*$^{-/-}$ mice in the indicated groups. Bar, 1 mm. (B) Maximal abdominal aortic diameter of *Sirt1*$^{flox/flox}$;*Apoe*$^{-/-}$ mice and SVKO;*Apoe*$^{-/-}$ mice in the indicated groups. n = 10–25. (C and D) Incidence of AAAs (C) and survival curve (D) of *Sirt1*$^{flox/flox}$;*Apoe*$^{-/-}$ mice and SVKO;*Apoe*$^{-/-}$ mice after AngII infusion. n = 19–25. (E) Total aortic weight-to-BW ratio of *Sirt1*$^{flox/flox}$;*Apoe*$^{-/-}$ mice and SVKO;*Apoe*$^{-/-}$ mice in the indicated groups. n = 10–15. (F and G) Representative images of EVG staining of abdominal aortic sections of *Sirt1*$^{flox/flox}$;*Apoe*$^{-/-}$ and SVKO;*Apoe*$^{-/-}$ mice (F) and semiquantitative analysis of elastin degradation (G). Bars: (top) 200 µm; (bottom) 100 µm. n = 6–8. All values are shown as the means ± SEM. *, P < 0.05; **, P < 0.01; ***, P < 0.001. P-values were obtained using a Fisher's exact test (C), by a log-rank (Mantel-Cox) test (D), by one-way ANOVA plus a Bonferroni test (G), or by a Kruskal-Wallis test plus a Dunn's multiple comparison test (B and E). F/F, flox/flox.

mice (Fig. 8, F–H). Additionally, ChIP against SIRT1 showed that AngII-treatment reduced the recruitment of SIRT1 onto the *Mmp2* promoter, particularly in the −669 to −485 bp region (Fig. 8, I and J). These results suggest that AngII infusion decreases SIRT1 deacetylase activity to increase H3K9ac levels on the *Mmp2* promoter, which may contribute to increased MMP2 expression in the aorta upon AngII infusion. All the results described in this section suggest that the CR-mediated increase in the aortic expression of SIRT1 may provide a prerequisite for lower histone H3K9ac levels on the *Mmp2* promoter, thereby preventing the increase in MMP2 expression after AngII infusion.

DISCUSSION

In the present study, we used a mouse model to determine that CR protects against AAA formation. We observed that 12 wk of CR remarkably reduced AngII-induced AAA formation in *Apoe*$^{-/-}$ mice. Furthermore, we observed a signif-

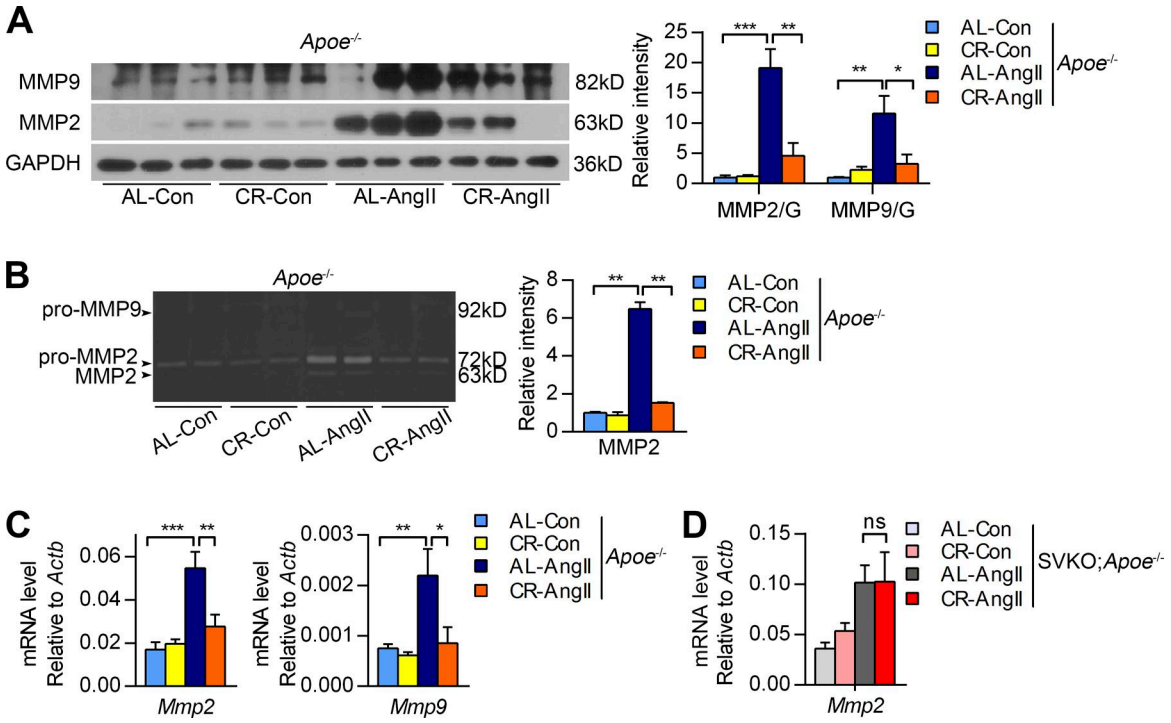

Figure 7. **CR reduces AngII-induced MMP2 expression and activity.** (A and B) Western blots (A) and gelatin zymography (B) of MMP2 and MMP9 in the aortas of *Apoe*$^{-/-}$ mice. Quantitative results are normalized to the AL-Con group values. $n = 4–6$ per group. (C) Relative mRNA expression of MMP2 and MMP9 in the aortas of *Apoe*$^{-/-}$ mice. $n = 6–12$ per group. (D) Relative mRNA expression of MMP2 in the aortas of SVKO;*Apoe*$^{-/-}$ mice. $n = 6–10$ per group. (C and D) Data were obtained from three independent experiments. All values are shown as the means ± SEM. *, $P < 0.05$; **, $P < 0.01$; ***, $P < 0.001$. P-values were obtained using a Kruskal-Wallis test plus a Dunn's multiple comparison test (A and B) or one-way ANOVA plus a Bonferroni posthoc analysis (C and D).

icant increase of VSMC-SIRT1 in aortas in response to CR. The smooth muscle–specific ablation of SIRT1 reduced the effectiveness of CR in preventing AAA. Our findings suggest a critical role for VSMC-SIRT1 in mediating the protective effects of CR on AAA formation.

As a calorie intake intervention, CR influences systemic metabolism. Consistent with previous studies (Guo et al., 2002; McCurdy and Cartee, 2005; Boily et al., 2008), in our mouse model, we observed that CR affected systemic metabolic indices by decreasing BW, EE, and RQ and improving glucose regulatory function. In addition to systemic metabolic changes, CR also reprograms local metabolism in different tissues, including the liver (Renaud et al., 2014), skeletal muscle (McCurdy and Cartee, 2005), and the heart (Sung et al., 2011). However, it remains unknown whether CR has an effect on glucose and lipid metabolism in the aorta. Although we observed an increase in the expression of key glycolysis and lipolysis enzymes and oxidative phosphorylation complex subunits in *Apoe*$^{-/-}$ mouse livers after CR, no significant alteration of these molecules was observed in aortas. Our findings suggest that despite the remarkable metabolic reprogramming in the liver, a 12-wk CR diet does not cause detectable changes in aortic glucose and lipid metabolism in *Apoe*$^{-/-}$ mice.

Although no significant metabolic changes were observed in the aortas upon CR, SIRT1 expression and activity was up-regulated in the aortas of *Apoe*$^{-/-}$ mice. In contrast, the expression of other metabolic/energy sensors, including SIRT3, AMPKα, and mTOR, was not significantly changed in the aortas. Furthermore, SIRT1 expression was significantly increased in VSMCs incubated with serum from CR mice. Studies from other groups have also demonstrated that serum from CR animals increases SIRT1 expression in human coronary artery endothelial cells and HEK293T cells (Cohen et al., 2004; Csiszar et al., 2009). These results indicate that SIRT1 is sensitive to circulating factors that are altered upon CR. A previous study has demonstrated that many metabolites, and lipids in particular, were altered in C57BL/6J mouse serum upon CR (Collino et al., 2013). Palmitic acid also reportedly decreases SIRT1 expression in human monocytes (THP-1) in vitro (de Kreutzenberg et al., 2010). Here, we observed that CR significantly decreased triglyceride levels in *Apoe*$^{-/-}$ mouse serum. Thus, the alteration of serum lipids by CR may contribute to SIRT1 up-regulation in the VSMCs of the aortic media. In addition, a recent study showed that [N^1]methylnicotinamide stabilizes SIRT1 to regulate hepatic metabolism (Hong et al., 2015). Hence, the changes of circulatory metabolites, such as [N^1]methylnicotinamide, may also contribute to the increase of vascular SIRT1 upon CR.

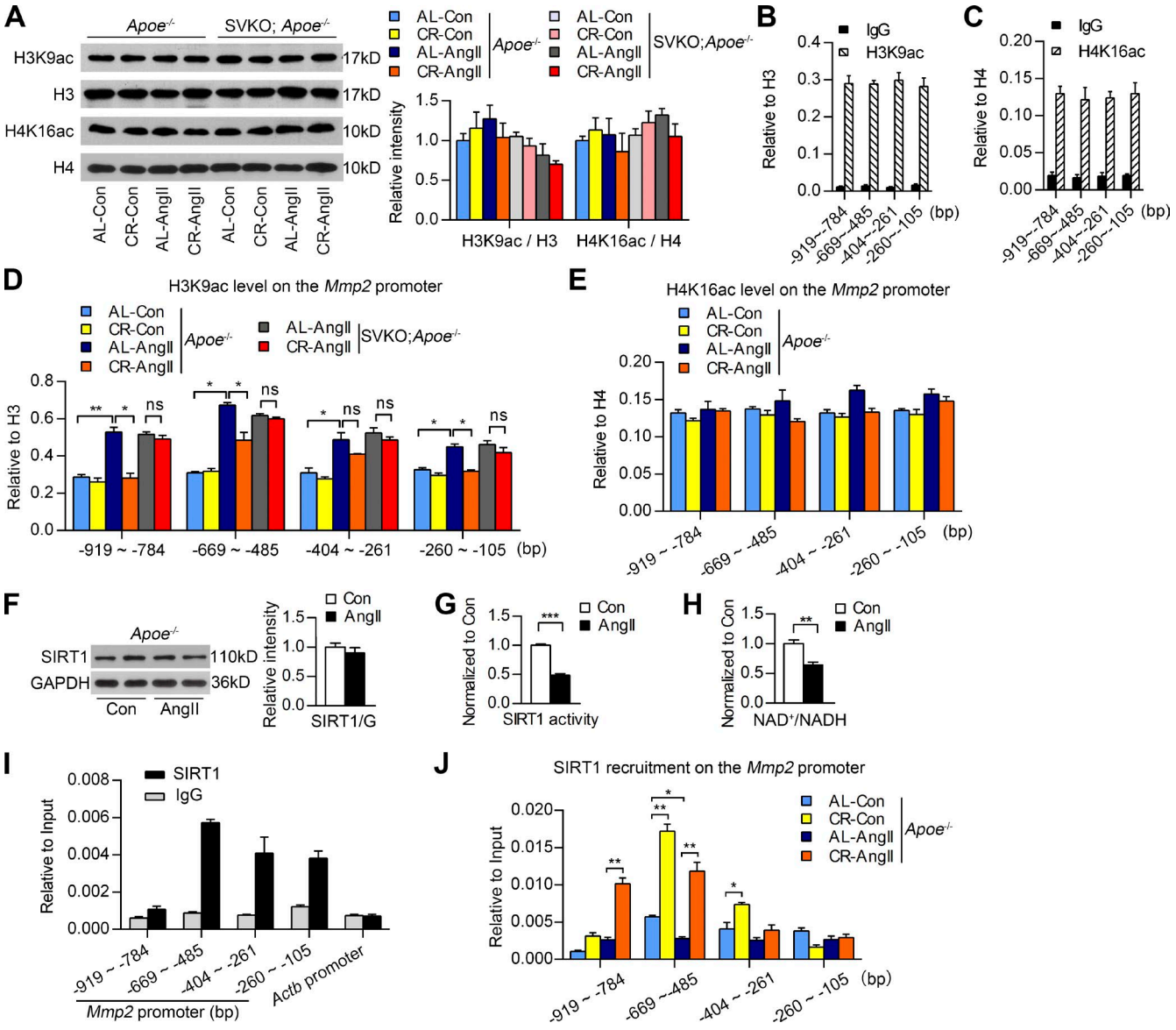

Figure 8. **CR attenuates AngII–induced MMP2 expression through VSMC-SIRT1–dependent H3K9 deacetylation in the *Mmp2* promoter.** (A, left) Western blots of H3K9 acetylation (H3K9ac), H3, H4K16ac, and H4 in aortas of *Apoe*$^{-/-}$ mice and SVKO;*Apoe*$^{-/-}$ mice. (Right) Densitometry was quantified and normalized to the AL-Con group. $n = 4$ per group. (B and C) ChIP of H3K9ac (B) and H4K16ac (C) on the *Mmp2* promoter in *Apoe*$^{-/-}$ mouse aortas. Four regions were detected: −919 ~ −784, −669 ~ −485, −404 ~ −261, and −260 ~ −105 bp. $n = 4$ per group. (D) ChIP assays of H3K9ac on the *Mmp2* promoter upon saline (Con) or AngII infusion. H3K9ac in the regions of −919 to −784, −669 to −485, −404 to −261, and −260 to −105 bp of the *Mmp2* promoter in the aortas of *Apoe*$^{-/-}$ and SVKO;*Apoe*$^{-/-}$ mice is shown. $n = 3$ per group. (E) ChIP of H4K16ac on the *Mmp2* promoter in aortic tissues of AL-Con, CR-Con, AL-AngII, and CR-AngII *Apoe*$^{-/-}$ mice. $n = 3$ per group. (F) Western blotting examination of aortic SIRT1 expression upon saline (Con) or AngII infusion for 4 wk in *Apoe*$^{-/-}$ mice. The quantification of Western blots is provided. $n = 3$ per group. (G and H) SIRT1 deacetylase activity (G) and NAD$^+$/NADH ratio (H) in the aortas of *Apoe*$^{-/-}$ mice in the indicated groups were examined. $n = 6$ per group. (I) SIRT1 enrichment in the *Mmp2* promoter was markedly higher than normal IgG in the aortas of AL-Con *Apoe*$^{-/-}$ mice. $n = 3$ per group. (J) SIRT1 enrichment in the regions of −919 to −784, −669 to −485, −404 to −261, and −260 to −105 bp of the *Mmp2* promoter in the aortas of *Apoe*$^{-/-}$ mice in the indicated groups. $n = 3$ per group. Three independent experiments were performed for ChIP assays. All values are shown as the means ± SEM. *, $P < 0.05$; **, $P < 0.01$; ***, $P < 0.001$. P-values were obtained using one-way ANOVA plus a Bonferroni posthoc analysis (A) or by an unpaired Student's *t* test with Welch's correction (B–J).

More importantly, we demonstrated that SIRT1 ablation in VSMCs reduced the preventive effect of CR on AAA formation but did not diminish the effect of CR on systemic metabolism. Although it remains to be elucidated exactly what metabolites mediate the up-regulation of VSMC-SIRT1 in response to CR, our findings suggest that VSMC-SIRT1

up-regulation is critical for the prevention of AngII-induced AAA formation during CR.

Epigenetic mechanisms underlie many aspects of the effects of CR on CVD prevention and health maintenance (Li et al., 2011b). As a metabolic sensor and a histone deacetylase, SIRT1 regulates CVDs by epigenetically regulating transcriptional factors and histones (Liu et al., 2014). Endothelial SIRT1 has been previously demonstrated to improve endothelial function and prevent atherosclerotic diseases by deacetylating H3K9 and H4K16 in target gene promoters (Zhou et al., 2011; Wan et al., 2014). However, it remains unclear whether SIRT1 in VSMCs participates in the epigenetic regulation of AAA formation. In the present study, we observed that VSMC-SIRT1 was a main sensor of CR in the aorta and that VSMC-SIRT1 was required for the CR-mediated prevention of AngII-induced AAA. MMP2 activation aggravated extracellular matrix degradation and promoted VSMC apoptosis, which is an important mechanism underlying AAA formation (Nataatmadja et al., 2003). We observed in the present study that CR suppressed the increase of *Mmp2* transcription and prevented the decrease of VSMC density in the aortas of $Apoe^{-/-}$ mice with AngII-induced AAAs. Moreover, the epigenetic regulation of MMP2 expression by SIRT1-dependent H3K9ac in the *Mmp2* promoter contributed to the CR-mediated inhibition of MMP2 expression after AngII infusion. VSMC-SIRT1 reportedly plays an important role in attenuating vascular remodeling by deacetylating transcription factors, thus regulating the expression of downstream molecules (Li et al., 2011a; Gao et al., 2014). MMP2 expression can be regulated by transcription factors such as NF-κB (Lin et al., 2010) and activator protein 1 (Bergman et al., 2003), which are also substrates of SIRT1 for deacetylation (Yeung et al., 2004; Zhang et al., 2010). Further studies will elucidate whether the modulation of transcription factors and histones by SIRT1 work in concert to regulate MMP2 expression in response to CR. In addition to the suppression of MMP2 expression and medial degradation, we also observed that CR decreased cytokine expression and 8-OHdG staining in the aortas of $Apoe^{-/-}$ mice after AngII infusion (unpublished data). These functions of CR may further contribute to protection against AAA progression.

In conclusion, the present study provides the first evidence that reducing calorie intake reduces AAA formation in mice. Moreover, VSMC-SIRT1 plays a critical role in mediating the protective effect of CR on AAA formation. Our findings support the benefit of a calorie-restricted lifestyle for AAA prevention and suggest that SIRT1 is a promising molecular target for the treatment of AAA.

MATERIALS AND METHODS

Animals

$Apoe^{-/-}$ mice on C57BL/6J background were obtained from Peking University. We established SVKO mice using a Cre/LoxP strategy. $Sirt1^{flox/flox}$ mice that expressed $SIRT1^{exon4}$ flanked by *LoxP* sites on the 129 background were purchased from The Jackson Laboratory (stock no. 008041). $SM22\alpha\text{-}Cre^{+/+}$ mice on the 129 background with a *Cre-recombinase* gene inserted into the endogenous *transgelin* (*SM22α*) locus were purchased from The Jackson Laboratory (stock no. 006878). These mice were backcrossed with mice on the C57BL/6J background for at least 10 generations to yield $Sirt1^{flox/flox}$ mice and $SM22\alpha\text{-}Cre^{+/-}$ mice on the C57BL/6J background. They were further crossed with $Apoe^{-/-}$ mice to generate $Sirt1^{flox/flox};Apoe^{-/-}$ and $SM22\alpha\text{-}Cre^{+/-};Apoe^{-/-}$ mice. Male $SM22\alpha\text{-}Cre^{+/-};Sirt1^{flox/flox};Apoe^{-/-}$ mice were crossed with female $Sirt1^{flox/flox};Apoe^{-/-}$ mice, both on the C57BL/6J background, to generate SVKO;$Apoe^{-/-}$ mice ($SM22\alpha\text{-}Cre^{+/-};Sirt1^{flox/flox};Apoe^{-/-}$). All of the mice were genotyped by PCR using tail clip samples. The primers used for genotyping are listed in Table S1. All of the animal protocols were approved by the Animal Care and Use Committee at the Institute of Basic Medical Sciences, Chinese Academy of Medical Sciences, and Peking Union Medical College.

CR and AAA mouse model

8-wk-old male $Apoe^{-/-}$ or SVKO;$Apoe^{-/-}$ mice were housed individually and randomly allocated into four groups. AL-Con mice and AL-AngII mice were fed AL with AL food for 16 wk. CR-Con mice and CR-AngII mice were fed a 10%-restricted diet for the first week and a 25%-restricted diet for the remaining experimental period of the CR diet. The AL and CR food were made according to the composition of AIN-93M, as previously described (Pugh et al., 1999). During the last 4 wk, AL-AngII and CR-AngII mice received subcutaneous AngII infusions in a dose of 1.44 mg/kg/d delivered via osmotic pumps (model 2004; Alzet). AL-Con and CR-Con mice received saline as a control. The detailed procedure was performed as previously described (Satoh et al., 2009). In the last week of the experiment, the mice underwent indirect calorimetry, IPGTT, and SBP measurement. After sacrifice, maximal diameters of suprarenal abdominal aortas and maximal diameters of ascending aortas were measured using Image Pro Plus software (Media Cybernetics) by a researcher blind to group assignment. AAA incidence was calculated based on a definition of aneurysm as an external width of the suprarenal aorta that was increased by ≥50% compared with aortas from saline-infused mice as previously described (Satoh et al., 2009).

Indirect calorimetry

Whole-body metabolic states of the mice were tested by indirect calorimetry in a comprehensive lab animal monitor system (Columbus Instruments) for 2 d after 1 d of habituation according to the manufacturer's instructions. Light and feeding conditions were kept the same as in the home cages. EE and RQ were calculated using the equations: EE (kcal/h) = $(3.818 \times VO_2) + (1.232 \times VCO_2)$ and $RQ = VO_2/VCO_2$. VO_2 stands for the volume of oxygen consumed per hour, and VCO_2 stands for the volume of carbon dioxide produced per hour. Because of the huge difference in BW between

the AL and CR mice, we compared their metabolic rates by normalizing to the metabolic size, as reflected by the $BW^{0.75}$ of each mouse (Zhou et al., 2012).

IPGTT

Before IPGTT, the mice were fasted overnight. Fasting blood glucose levels were measured with blood that was collected via tail tip cutting using a portable glucose meter (Yuyue). Mice were injected intraperitoneally with 2 g/kg BW D-glucose dissolved in saline, and blood glucose levels were measured at 15, 30, 60, and 120 min after glucose injection.

SBP measurement

SBP was measured in the last week of AngII infusion. SBP was measured using tail-cuff plethysmography (BP-2000 System; Visitech Systems) as previously described (Li et al., 2011a).

Mouse serum collection and serum lipid measurement

Mice were fasted overnight and anesthetized before blood collection. Blood was collected from the abdominal vena cava before euthanasia, allowed to clot for 20–30 min, and centrifuged at 3,000 *g* for 20 min. Serum was collected from the centrifuged samples and stored at −70°C until use. The serum was thawed, and triglyceride and cholesterol levels were measured at the Peking Union Medical College Hospital clinical laboratory.

EVG, IF, and IHC staining

After the mice were executed, aortas from the ascending aorta to the furcation of the common iliac artery were isolated. After macroscopic analysis, suprarenal abdominal aortas were subjected to histology analysis. The aortas and adventitia were fixed with 4% paraformaldehyde-PBS for 24 h and embedded in paraffin, and serial sections were made using suprarenal abdominal aortas and four sections (5 µm each) at 500-µm intervals as previously described (Satoh et al., 2009). Paraffin sections were stained with EVG or used for IF staining and IHC staining. The grade of elastin degradation was quantified by a researcher who was blinded to the group assignment according to the criteria previously described (Satoh et al., 2009). The grades were as follows: score 1, no degradation; score 2, mild elastin degradation; score 3, severe elastin degradation; and score 4, aortic rupture. The primary antibodies used in IF and IHC staining were αSMA (A2547, Sigma-Aldrich; ab5694, Abcam) and SIRT1 (07-131; EMD Millipore). The secondary antibodies used in IF staining were Alexa Fluor 488–conjugated goat anti–mouse IgG and Alexa Fluor 594–conjugated goat anti–rabbit IgG. Nuclei were stained with Hoechst Stain solution (B2261; Sigma-Aldrich). All of the pictures were taken with the same settings.

Relative mRNA quantification

Total RNA was extracted using TRIzol reagent (Invitrogen) and first-strand cDNA was synthesized from 3 µg RNA using a reverse transcription system (New England Biolabs, Inc.) according to the manufacturer's instructions. Quantitative real-time PCR was performed using Green Premix Ex Taq reagent (Takara Bio Inc.) on a Mastercycler machine (Eppendorf) with cDNA as a template. Primers were designed to span exon boundaries to avoid genomic DNA amplification. Target mRNA expression was calculated relative to *Actb*. Primer sequences are provided in Table S2.

Western blotting

Western blotting was performed as previously described (Zhou et al., 2011). The primary antibodies used were SIRT1 (07-131; EMD Millipore), SIRT3 (5490; Cell Signaling Technology), AMPKα (9957; Cell Signaling Technology), phosphorylated AMPKα (9957; Cell Signaling Technology), mTOR (2983; Cell Signaling Technology), phosphorylated mTOR (2971; Cell Signaling Technology), GAPDH (5174; Cell Signaling Technology), MMP2 (sc13595; Santa Cruz Biotechnology, Inc.), MMP9 (ab38898; Abcam), H3K9ac (ab10812; Abcam), H3 (ab1791; Abcam), H4K16ac (07-329; EMD Millipore), and H4 (05-858; EMD Millipore). Western blots were quantified densitometrically using Image Pro-Plus software (Media Cybernetics), the intensity values were calculated relative to GAPDH, H3, or H4, and the values were normalized to AL-Con values.

SIRT1 activity assay

Freshly isolated mouse aortas were homogenized with immunoprecipitation buffer (P0013; Beyotime Biotechnology). SIRT1 was immunoprecipitated with SIRT1 antibodies (07-131; EMD Millipore) from whole aortic homogenates (200 µg protein). Aortic SIRT1 activity was assessed using a SIRT1 deacetylase activity assay kit (CS1040; Sigma-Aldrich) according to the manufacturer's instructions.

NAD^+/NADH level measurement

Freshly isolated mouse aortas were used for measuring aortic NAD^+/NADH levels following the manufacturer's instructions (ab65348; Abcam).

VSMC culture and mouse serum incubation

VSMCs for culture were isolated from suprarenal abdominal aortas of 2–3-mo-old 20–25-g WT male mice and maintained in DMEM containing 10% FBS at 37°C in a humidified atmosphere of 5% CO_2 and 95% air, as previously described (Ishida et al., 1999). Four to five passages of VSMCs at 70–80% confluence were incubated in DMEM containing 10% serum from AL-Con or CR-Con *Apoe*$^{-/-}$ mice for 48 h. Mouse serum was thawed and heat inactivated at 56°C for 30 min before use in cell culture experiments.

Gelatin zymography

MMP activity was measured as previously reported (Hawkes et al., 2010). Aortic homogenates (5 µg protein) were electrophoresed in SDS-PAGE gels containing gelatin. The gels were washed in 2.5% Triton X-100 for 30 min and incubated for

12–40 h in zymography development buffer (0.05 M Tris-HCl, pH 8.8, 5 mM $CaCl_2$, and 0.02% NaN_3) at 37°C. The gels were subsequently stained with Coomassie brilliant blue.

Tissue ChIP assay

Freshly isolated mouse aortas were carefully stripped out of the adventitial layer and chopped into small pieces. Aortic tissue was digested with 0.05% trypsin-EDTA (BRL 25300; Gibco) for 5 min at 37°C, followed by the addition of 9 ml of 10% FBS-DMEM to stop digestion. ChIP assays were performed using aortic tissues as previously described (Wang et al., 2008). The antibodies used in ChIP included anti-H3 (ab1791; Abcam), H3K9ac (ab10812; Abcam), H4 (05-858; EMD Millipore), H4K16ac (07-329; EMD Millipore), SIRT1 (07-131; EMD Millipore), and normal rabbit IgG (sc-2027; Santa Cruz Biotechnology, Inc.). DNA was detected by quantitative real-time PCR. Specific primers were designed to amplify the *Mmp2* promoter. The primer sequences are provided in Table S3.

Statistical analysis

Quantitative results are expressed as the means ± SEM. The normality and the homogeneity of variance of the data were tested. To compare among three or more groups, a one-way ANOVA plus a posthoc analysis (Bonferroni test) was used for normally distributed variables, and a Kruskal-Wallis test plus a posthoc analysis (Dunn's multiple comparison test) was used for variables not passing a normality or equal variance test. Two-way repeated-measures ANOVA was used for BW data and IPGTT data that were repeatedly measured. Fisher's exact test was applied to the comparisons of aneurysm incidence. The log-rank (Mantel-Cox) test was used for survival analysis. All statistical analyses were performed using Prism 6.0 (GraphPad Software). A p-value <0.05 was considered to be statistically significant.

Online supplemental material

Table S1 shows primers used for genotyping. Table S2 shows primers used for measuring relative mRNA expression. Table S3 shows primers used in tissue ChIP assays.

ACKNOWLEDGMENTS

This work is supported by grants from the National Natural Science Foundation of China (91339201, 81422002, 31571193, and 31271227) and the National Basic Research Program of China (2011CB503902).

The authors declare no competing financial interests.

Submitted: 15 November 2015

Accepted: 26 August 2016

REFERENCES

Bergman, M.R., S. Cheng, N. Honbo, L. Piacentini, J.S. Karliner, and D.H. Lovett. 2003. A functional activating protein 1 (AP-1) site regulates matrix metalloproteinase 2 (MMP-2) transcription by cardiac cells through interactions with JunB-Fra1 and JunB-FosB heterodimers. *Biochem. J.* 369:485–496. http://dx.doi.org/10.1042/bj20020707

Blagosklonny, M.V. 2010. Calorie restriction: decelerating mTOR-driven aging from cells to organisms (including humans). *Cell Cycle.* 9:683–688. http://dx.doi.org/10.4161/cc.9.4.10766

Boily, G., E.L. Seifert, L. Bevilacqua, X.H. He, G. Sabourin, C. Estey, C. Moffat, S. Crawford, S. Saliba, K. Jardine, et al. 2008. SirT1 regulates energy metabolism and response to caloric restriction in mice. *PLoS One.* 3:e1759. http://dx.doi.org/10.1371/journal.pone.0001759

Bown, M.J., M.J. Sweeting, L.C. Brown, J.T. Powell, and S.G. Thompson. RESCAN Collaborators. 2013. Surveillance intervals for small abdominal aortic aneurysms: a meta-analysis. *JAMA.* 309:806–813. http://dx.doi.org/10.1001/jama.2013.950

Cantó, C., and J. Auwerx. 2011. Calorie restriction: is AMPK a key sensor and effector? *Physiology (Bethesda).* 26:214–224. http://dx.doi.org/10.1152/physiol.00010.2011

Cerletti, M., Y.C. Jang, L.W. Finley, M.C. Haigis, and A.J. Wagers. 2012. Short-term calorie restriction enhances skeletal muscle stem cell function. *Cell Stem Cell.* 10:515–519. http://dx.doi.org/10.1016/j.stem.2012.04.002

Cohen, H.Y., C. Miller, K.J. Bitterman, N.R. Wall, B. Hekking, B. Kessler, K.T. Howitz, M. Gorospe, R. de Cabo, and D.A. Sinclair. 2004. Calorie restriction promotes mammalian cell survival by inducing the SIRT1 deacetylase. *Science.* 305:390–392. http://dx.doi.org/10.1126/science.1099196

Collino, S., F.P. Martin, I. Montoliu, J.L. Barger, L. Da Silva, T.A. Prolla, R. Weindruch, and S. Kochhar. 2013. Transcriptomics and metabonomics identify essential metabolic signatures in calorie restriction (CR) regulation across multiple mouse strains. *Metabolites.* 3:881–911. http://dx.doi.org/10.3390/metabo3040881

Colman, R.J., R.M. Anderson, S.C. Johnson, E.K. Kastman, K.J. Kosmatka, T.M. Beasley, D.B. Allison, C. Cruzen, H.A. Simmons, J.W. Kemnitz, and R. Weindruch. 2009. Caloric restriction delays disease onset and mortality in rhesus monkeys. *Science.* 325:201–204. http://dx.doi.org/10.1126/science.1173635

Colman, R.J., T.M. Beasley, J.W. Kemnitz, S.C. Johnson, R. Weindruch, and R.M. Anderson. 2014. Caloric restriction reduces age-related and all-cause mortality in rhesus monkeys. *Nat. Commun.* 5:3557. http://dx.doi.org/10.1038/ncomms4557

Csiszar, A., N. Labinskyy, R. Jimenez, J.T. Pinto, P. Ballabh, G. Losonczy, K.J. Pearson, R. de Cabo, and Z. Ungvari. 2009. Anti-oxidative and anti-inflammatory vasoprotective effects of caloric restriction in aging: role of circulating factors and SIRT1. *Mech. Ageing Dev.* 130:518–527. http://dx.doi.org/10.1016/j.mad.2009.06.004

Daugherty, A., and L.A. Cassis. 2004. Mouse models of abdominal aortic aneurysms. *Arterioscler. Thromb. Vasc. Biol.* 24:429–434. http://dx.doi.org/10.1161/01.ATV.0000118013.72016.ea

Daugherty, A., M.W. Manning, and L.A. Cassis. 2000. Angiotensin II promotes atherosclerotic lesions and aneurysms in apolipoprotein E-deficient mice. *J. Clin. Invest.* 105:1605–1612. http://dx.doi.org/10.1172/JCI7818

Daugherty, A., D.L. Rateri, I.F. Charo, A.P. Owens, D.A. Howatt, and L.A. Cassis. 2010. Angiotensin II infusion promotes ascending aortic aneurysms: attenuation by CCR2 deficiency in apoE$^{-/-}$ mice. *Clin. Sci.* 118:681–689. http://dx.doi.org/10.1042/CS20090372

de Kreutzenberg, S.V., G. Ceolotto, I. Papparella, A. Bortoluzzi, A. Semplicini, C. Dalla Man, C. Cobelli, G.P. Fadini, and A. Avogaro. 2010. Downregulation of the longevity-associated protein sirtuin 1 in insulin resistance and metabolic syndrome: potential biochemical mechanisms. *Diabetes.* 59:1006–1015. http://dx.doi.org/10.2337/db09-1187

Fontana, L., T.E. Meyer, S. Klein, and J.O. Holloszy. 2004. Long-term calorie restriction is highly effective in reducing the risk for atherosclerosis in humans. *Proc. Natl. Acad. Sci. USA.* 101:6659–6663. http://dx.doi.org/10.1073/pnas.0308291101

Fontana, L., D.T. Villareal, E.P. Weiss, S.B. Racette, K. Steger-May, S. Klein, and J.O. Holloszy. Washington University School of Medicine CALERIE Group. 2007. Calorie restriction or exercise: effects on coronary

heart disease risk factors. A randomized, controlled trial. *Am. J. Physiol. Endocrinol. Metab.* 293:E197–E202. http://dx.doi.org/10.1152/ajpendo.00102.2007

Fontana, L., L. Partridge, and V.D. Longo. 2010. Extending healthy life span—from yeast to humans. *Science.* 328:321–326. http://dx.doi.org/10.1126/science.1172539

Gao, P., T.T. Xu, J. Lu, L. Li, J. Xu, D.L. Hao, H.Z. Chen, and D.P. Liu. 2014. Overexpression of SIRT1 in vascular smooth muscle cells attenuates angiotensin II-induced vascular remodeling and hypertension in mice. *J. Mol. Med.* 92:347–357. http://dx.doi.org/10.1007/s00109-013-1111-4

Golledge, J., P. Clancy, K. Jamrozik, and P.E. Norman. 2007. Obesity, adipokines, and abdominal aortic aneurysm: Health in men study. *Circulation.* 116:2275–2279. http://dx.doi.org/10.1161/CIRCULATIONAHA.107.717926

Gorenne, I., S. Kumar, K. Gray, N. Figg, H.Yu, J. Mercer, and M. Bennett. 2013. Vascular smooth muscle cell sirtuin 1 protects against DNA damage and inhibits atherosclerosis. *Circulation.* 127:386–396. http://dx.doi.org/10.1161/CIRCULATIONAHA.112.124404

Guarente, L. 2013. Calorie restriction and sirtuins revisited. *Genes Dev.* 27:2072–2085. http://dx.doi.org/10.1101/gad.227439.113

Guo, Z., F. Mitchell-Raymundo, H. Yang, Y. Ikeno, J. Nelson, V. Diaz, A. Richardson, and R. Reddick. 2002. Dietary restriction reduces atherosclerosis and oxidative stress in the aorta of apolipoprotein E-deficient mice. *Mech. Ageing Dev.* 123:1121–1131. http://dx.doi.org/10.1016/S0047-6374(02)00008-8

Hallows, W.C., W. Yu, B.C. Smith, M.K. Devries, J.J. Ellinger, S. Someya, M.R. Shortreed, T. Prolla, J.L. Markley, L.M. Smith, et al. 2011. Sirt3 promotes the urea cycle and fatty acid oxidation during dietary restriction. *Mol. Cell.* 41:139–149. http://dx.doi.org/10.1016/j.molcel.2011.01.002

Hawkes, S.P., H. Li, and G.T. Taniguchi. 2010. Zymography and reverse zymography for detecting MMPs and TIMPs. *Methods Mol. Biol.* 622:257–269. http://dx.doi.org/10.1007/978-1-60327-299-5_16

Hong, S., J.M. Moreno-Navarrete, X. Wei, Y. Kikukawa, I. Tzameli, D. Prasad, Y. Lee, J.M. Asara, J.M. Fernandez-Real, E. Maratos-Flier, and P. Pissios. 2015. Nicotinamide N-methyltransferase regulates hepatic nutrient metabolism through Sirt1 protein stabilization. *Nat. Med.* 21:887–894. http://dx.doi.org/10.1038/nm.3882

Ishida, T., M. Ishida, J. Suero, M. Takahashi, and B.C. Berk. 1999. Agonist-stimulated cytoskeletal reorganization and signal transduction at focal adhesions in vascular smooth muscle cells require c-Src. *J. Clin. Invest.* 103:789–797. http://dx.doi.org/10.1172/JCI4189

Johnston, K.W., R.B. Rutherford, M.D. Tilson, D.M. Shah, L. Hollier, and J.C. Stanley. 1991. Suggested standards for reporting on arterial aneurysms. *J. Vasc. Surg.* 13:452–458. http://dx.doi.org/10.1067/mva.1991.26737

Lederle, F.A. 2013. Abdominal aortic aneurysm: still no pill. *Ann. Intern. Med.* 159:852–853. http://dx.doi.org/10.7326/0003-4819-159-12-201312170-00012

Lee, C.K., R.G. Klopp, R. Weindruch, and T.A. Prolla. 1999. Gene expression profile of aging and its retardation by caloric restriction. *Science.* 285:1390–1393. http://dx.doi.org/10.1126/science.285.5432.1390

Lefevre, M., L.M. Redman, L.K. Heilbronn, J.V. Smith, C.K. Martin, J.C. Rood, F.L. Greenway, D.A. Williamson, S.R. Smith, and E. Ravussin. Pennington CALERIE team. 2009. Caloric restriction alone and with exercise improves CVD risk in healthy non-obese individuals. *Atherosclerosis.* 203:206–213. http://dx.doi.org/10.1016/j.atherosclerosis.2008.05.036

Li, L., H.N. Zhang, H.Z. Chen, P. Gao, L.H. Zhu, H.L. Li, X. Lv, Q.J. Zhang, R. Zhang, Z. Wang, et al. 2011a. SIRT1 acts as a modulator of neointima formation following vascular injury in mice. *Circ. Res.* 108:1180–1189. http://dx.doi.org/10.1161/CIRCRESAHA.110.237875

Li, Y., M. Daniel, and T.O. Tollefsbol. 2011b. Epigenetic regulation of caloric restriction in aging. *BMC Med.* 9:98. http://dx.doi.org/10.1186/1741-7015-9-98

Lin, M.L., Y.C. Lu, J.G. Chung, S.G. Wang, H.T. Lin, S.E. Kang, C.H. Tang, J.L. Ko, and S.S. Chen. 2010. Down-regulation of MMP-2 through the p38 MAPK-NF-κB-dependent pathway by aloe-emodin leads to inhibition of nasopharyngeal carcinoma cell invasion. *Mol. Carcinog.* 49:783–797. http://dx.doi.org/10.1002/mc.20652

Liu, Y., H. Chen, and D. Liu. 2014. Mechanistic perspectives of calorie restriction on vascular homeostasis. *Sci. China Life Sci.* 57:742–754. http://dx.doi.org/10.1007/s11427-014-4709-z

Logan, A.J., and N.I. Bourantas. 2000. Mortality from ruptured abdominal aortic aneurysm in Wales. *Br. J. Surg.* 87:966–967.

Longo, G.M., W. Xiong, T.C. Greiner, Y. Zhao, N. Fiotti, and B.T. Baxter. 2002. Matrix metalloproteinases 2 and 9 work in concert to produce aortic aneurysms. *J. Clin. Invest.* 110:625–632. http://dx.doi.org/10.1172/JCI0215334

López-Candales, A., D.R. Holmes, S. Liao, M.J. Scott, S.A. Wickline, and R.W. Thompson. 1997. Decreased vascular smooth muscle cell density in medial degeneration of human abdominal aortic aneurysms. *Am. J. Pathol.* 150:993–1007.

McCurdy, C.E., and G.D. Cartee. 2005. Akt2 is essential for the full effect of calorie restriction on insulin-stimulated glucose uptake in skeletal muscle. *Diabetes.* 54:1349–1356. http://dx.doi.org/10.2337/diabetes.54.5.1349

Nataatmadja, M., M. West, J. West, K. Summers, P. Walker, M. Nagata, and T. Watanabe. 2003. Abnormal extracellular matrix protein transport associated with increased apoptosis of vascular smooth muscle cells in marfan syndrome and bicuspid aortic valve thoracic aortic aneurysm. *Circulation.* 108:II329–II334. http://dx.doi.org/10.1161/01.cir.0000087660.82721.15

Nordon, I.M., R.J. Hinchliffe, I.M. Loftus, and M.M. Thompson. 2011. Pathophysiology and epidemiology of abdominal aortic aneurysms. *Nat. Rev. Cardiol.* 8:92–102. http://dx.doi.org/10.1038/nrcardio.2010.180

Piper, M.D., and A. Bartke. 2008. Diet and aging. *Cell Metab.* 8:99–104. http://dx.doi.org/10.1016/j.cmet.2008.06.012

Police, S.B., S.E. Thatcher, R. Charnigo, A. Daugherty, and L.A. Cassis. 2009. Obesity promotes inflammation in periaortic adipose tissue and angiotensin II-induced abdominal aortic aneurysm formation. *Arterioscler. Thromb. Vasc. Biol.* 29:1458–1464. http://dx.doi.org/10.1161/ATVBAHA.109.192658

Police, S.B., K. Putnam, S. Thatcher, F. Batifoulier-Yiannikouris, A. Daugherty, and L.A. Cassis. 2010. Weight loss in obese C57BL/6 mice limits adventitial expansion of established angiotensin II-induced abdominal aortic aneurysms. *Am. J. Physiol. Heart Circ. Physiol.* 298:H1932–H1938. http://dx.doi.org/10.1152/ajpheart.00961.2009

Pugh, T.D., R.G. Klopp, and R. Weindruch. 1999. Controlling caloric consumption: protocols for rodents and rhesus monkeys. *Neurobiol. Aging.* 20:157–165. http://dx.doi.org/10.1016/S0197-4580(99)00043-3

Renaud, H.J., J.Y. Cui, H. Lu, and C.D. Klaassen. 2014. Effect of diet on expression of genes involved in lipid metabolism, oxidative stress, and inflammation in mouse liver-insights into mechanisms of hepatic steatosis. *PLoS One.* 9:e88584. http://dx.doi.org/10.1371/journal.pone.0088584

Ryall, J.G., S. Dell'Orso, A. Derfoul, A. Juan, H. Zare, X. Feng, D. Clermont, M. Koulnis, G. Gutierrez-Cruz, M. Fulco, and V. Sartorelli. 2015. The NAD^+-dependent SIRT1 deacetylase translates a metabolic switch into regulatory epigenetics in skeletal muscle stem cells. *Cell Stem Cell.* 16:171–183. http://dx.doi.org/10.1016/j.stem.2014.12.004

Satoh, K., P. Nigro, T. Matoba, M.R. O'Dell, Z. Cui, X. Shi, A. Mohan, C. Yan, J. Abe, K.A. Illig, and B.C. Berk. 2009. Cyclophilin A enhances vascular oxidative stress and the development of angiotensin II-induced aortic aneurysms. *Nat. Med.* 15:649–656. http://dx.doi.org/10.1038/nm.1958

Stackelberg, O., M. Björck, O. Sadr-Azodi, S.C. Larsson, N. Orsini, and A. Wolk. 2013. Obesity and abdominal aortic aneurysm. *Br. J. Surg.* 100:360–366. http://dx.doi.org/10.1002/bjs.8983

Strom, A., and R.A. Jensen. 1951. Mortality from circulatory diseases in Norway 1940-1945. *Lancet*. 1:126–129. http://dx.doi.org/10.1016/S0140-6736(51)91210-X

Sung, M.M., C.L. Soltys, G. Masson, J.J. Boisvenue, and J.R. Dyck. 2011. Improved cardiac metabolism and activation of the RISK pathway contributes to improved post-ischemic recovery in calorie restricted mice. *J. Mol. Med*. 89:291–302. http://dx.doi.org/10.1007/s00109-010-0703-5

Taylor, G.C., R. Eskeland, B. Hekimoglu-Balkan, M.M. Pradeepa, and W.A. Bickmore. 2013. H4K16 acetylation marks active genes and enhancers of embryonic stem cells, but does not alter chromatin compaction. *Genome Res.* 23:2053–2065. http://dx.doi.org/10.1101/gr.155028.113

Trivedi, D.B., C.D. Loftin, J. Clark, P. Myers, L.M. DeGraff, J. Cheng, D.C. Zeldin, and R. Langenbach. 2013. β-Arrestin-2 deficiency attenuates abdominal aortic aneurysm formation in mice. *Circ. Res.* 112:1219–1229. http://dx.doi.org/10.1161/CIRCRESAHA.112.280399

Vaquero, A., M. Scher, D. Lee, H. Erdjument-Bromage, P. Tempst, and D. Reinberg. 2004. Human SirT1 interacts with histone H1 and promotes formation of facultative heterochromatin. *Mol. Cell*. 16:93–105. http://dx.doi.org/10.1016/j.molcel.2004.08.031

Verhoeven, E.L., M.R. Kapma, H. Groen, I.F. Tielliu, C.J. Zeebregts, F. Bekkema, and J.J. van den Dungen. 2008. Mortality of ruptured abdominal aortic aneurysm treated with open or endovascular repair. *J. Vasc. Surg.* 48:1396–1400. http://dx.doi.org/10.1016/j.jvs.2008.07.054

Wan, Y.Z., P. Gao, S. Zhou, Z.Q. Zhang, D.L. Hao, L.S. Lian, Y.J. Li, H.Z. Chen, and D.P. Liu. 2014. SIRT1-mediated epigenetic downregulation of plasminogen activator inhibitor-1 prevents vascular endothelial replicative senescence. *Aging Cell*. 13:890–899. http://dx.doi.org/10.1111/acel.12247

Wang, R.H., Y. Zheng, H.S. Kim, X. Xu, L. Cao, T. Luhasen, M.H. Lee, C. Xiao, A. Vassilopoulos, W. Chen, et al. 2008. Interplay among BRCA1, SIRT1, and Survivin during BRCA1-associated tumorigenesis. *Mol. Cell*. 32:11–20. http://dx.doi.org/10.1016/j.molcel.2008.09.011

Wang, Y., H. Ait-Oufella, O. Herbin, P. Bonnin, B. Ramkhelawon, S. Taleb, J. Huang, G. Offenstadt, C. Combadière, L. Rénia, et al. 2010. TGF-β activity protects against inflammatory aortic aneurysm progression and complications in angiotensin II–infused mice. *J. Clin. Invest.* 120:422–432. http://dx.doi.org/10.1172/JCI38136

Weiss, E.P., and J.O. Holloszy. 2007. Improvements in body composition, glucose tolerance, and insulin action induced by increasing energy expenditure or decreasing energy intake. *J. Nutr.* 137:1087–1090.

Weiss, E.P., S.B. Racette, D.T. Villareal, L. Fontana, K. Steger-May, K.B. Schechtman, S. Klein, and J.O. Holloszy. Washington University School of Medicine CALERIE Group. 2006. Improvements in glucose tolerance and insulin action induced by increasing energy expenditure or decreasing energy intake: a randomized controlled trial. *Am. J. Clin. Nutr.* 84:1033–1042.

Willcox, B.J., D.C. Willcox, H. Todoriki, A. Fujiyoshi, K. Yano, Q. He, J.D. Curb, and M. Suzuki. 2007. Caloric restriction, the traditional Okinawan diet, and healthy aging: the diet of the world's longest-lived people and its potential impact on morbidity and life span. *Ann. N. Y. Acad. Sci.* 1114:434–455. http://dx.doi.org/10.1196/annals.1396.037

Yeung, F., J.E. Hoberg, C.S. Ramsey, M.D. Keller, D.R. Jones, R.A. Frye, and M.W. Mayo. 2004. Modulation of NF-κB-dependent transcription and cell survival by the SIRT1 deacetylase. *EMBO J.* 23:2369–2380. http://dx.doi.org/10.1038/sj.emboj.7600244

Zhang, R., H.Z. Chen, J.J. Liu, Y.Y. Jia, Z.Q. Zhang, R.F. Yang, Y. Zhang, J. Xu, Y.S. Wei, D.P. Liu, and C.C. Liang. 2010. SIRT1 suppresses activator protein-1 transcriptional activity and cyclooxygenase-2 expression in macrophages. *J. Biol. Chem.* 285:7097–7110. http://dx.doi.org/10.1074/jbc.M109.038604

Zhou, B., L. Yang, S. Li, J. Huang, H. Chen, L. Hou, J. Wang, C.D. Green, Z. Yan, X. Huang, et al. 2012. Midlife gene expressions identify modulators of aging through dietary interventions. *Proc. Natl. Acad. Sci. USA*. 109:E1201–E1209. http://dx.doi.org/10.1073/pnas.1119304109

Zhou, S., H.Z. Chen, Y.Z. Wan, Q.J. Zhang, Y.S. Wei, S. Huang, J.J. Liu, Y.B. Lu, Z.Q. Zhang, R.F. Yang, et al. 2011. Repression of P66Shc expression by SIRT1 contributes to the prevention of hyperglycemia-induced endothelial dysfunction. *Circ. Res.* 109:639–648. http://dx.doi.org/10.1161/CIRCRESAHA.111.243592